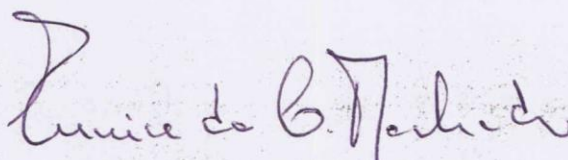


*"Inventory of Carbon in a Subtropical Estuary"*

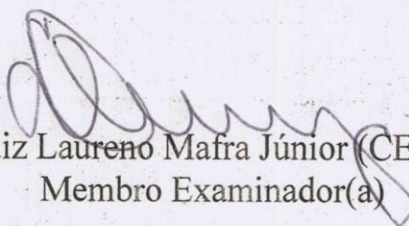
POR

Bruno Guides Libardoni

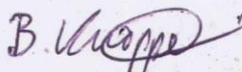
Dissertação nº 114 aprovada como requisito parcial do grau de Mestre(a) no Curso de Pós-Graduação em Sistemas Costeiros e Oceânicos da Universidade Federal do Paraná, pela Comissão formada pelos professores:



Dr(a). Eunice da Costa Machado  
Orientador(a) e Presidente(a)



Dr(a). Luiz Laurenô Mafra Júnior (CEM-UFPR)  
Membro Examinador(a)



Dr(a). Bastiaan Knoppers (UFF)  
Membro Examinador(a)

Pontal do Paraná, 05/2/2014.

CATALOGAÇÃO NA FONTE:  
UFPR / SIBI - Biblioteca do Centro de Estudos do Mar

L694i Libardoni, Bruno Guides  
Inventory of carbon in a subtropical estuarine system / Bruno Guides Libardoni. –  
Pontal do Paraná, 2014.  
49 f.; 29 cm.

Orientadores: Prof. Dra. Eunice da Costa Machado  
Prof. Dr. Tom Moens

Dissertação (Mestrado) – Programa de Pós-graduação em Sistemas Costeiros  
e Oceânicos, Centro de Estudos do Mar, Setor de Ciências da Terra, Universidade  
Federal do Paraná.

1. Carbon. 2. Estuary. 3. Subtropical. 4. Fluxes. 5. Alkalinity. I. Título. II.  
Machado, Eunice da Costa. III. Universidade Federal do Paraná.

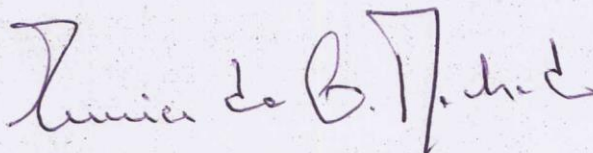
CDD 551.466

## TERMO DE APROVAÇÃO

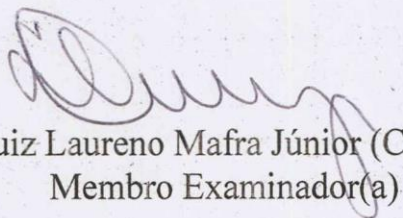
Bruno Guides Libardoni

### *Inventory of Carbon in a Subtropical Estuary*

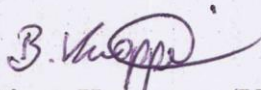
Dissertação aprovada como requisito parcial para a obtenção do grau de Mestre(a) em Sistemas Costeiros e Oceânicos, da Universidade Federal do Paraná, pela Comissão formada pelos professores:



Dr(a). Eunice da Costa Machado  
Orientador(a) e Presidente(a)



Dr(a). Luiz Laureno Mafra Júnior (CEM-UFPR)  
Membro Examinador(a)



Dr(a). Bastiaan Knoppers (UFF)  
Membro Examinador(a)

Pontal do Paraná, 05/2/2014.

UNIVERSIDADE FEDERAL DO PARANÁ

BRUNO GUIDES LIBARDONI

INVENTORY OF CARBON IN A SUBTROPICAL ESTUARINE SYSTEM

PONTAL DO PARANÁ

2014

BRUNO GUIDES LIBARDONI

INVENTORY OF CARBON IN A SUBTROPICAL ESTUARINE SYSTEM

Dissertação apresentada como requisito parcial à conclusão do curso de Pós Graduação em Sistemas Costeiros e Oceânicos, Centro de Estudos do Mar, Setor de Ciências da Terra, Universidade Federal do Paraná.

Orientadores: Prof<sup>a</sup>. Dra. Eunice da Costa Machado e Prof. Dr. Tom Moens.

PONTAL DO PARANÁ

2014

## RESUMO

As variações das fontes de carbono orgânico e suas variações espaciais são importantes para compreender o balanço das diferentes formas de carbono orgânico nas regiões costeiras. Amostragens foram feitas ao longo de gradientes de salinidade e nas duas desembocaduras do Complexo Estuarino de Paranaguá (CEP), objetivando analisar a distribuição espacial do Carbono Orgânico Particulado (COP) e do Carbono Orgânico Dissolvido (COD), as variações das saturações do  $\text{CO}_2$  e  $\text{O}_2$ , análises metabólicas do estuário, fluxos de difusão do  $\text{CO}_2$  e as exportações do COP e do COD para a área costeira adjacente ao CEP. O sistema está localizado no estado do Paraná, região sul do Brasil, compreendendo uma área de  $612\text{km}^2$  e um volume de  $2 \times 10^9\text{m}^3$ . Amostras foram coletadas durante campanhas amostras, ao longo de gradientes de salinidade dos eixos Norte-Sul e Leste-Oeste, e nas desembocaduras Norte e Sul do sistema. As amostras de carbono orgânico foram analisadas através do método de combustão em alta temperatura HTC no equipamento TOC-5000 Shimadzu; os fluxos de difusão, na interface ar-água foram estimados de acordo com Carmouze (1994) e as exportações foram baseadas em fundeios de medição como equipamento S4 Current Meter, medindo as correntes e descargas de água durante um ciclo completo de maré. Os resultados apresentaram variações nos valores de concentração de carbono orgânico: máximo de  $13.56\text{mg.L}^{-1}$ , mínimo de  $3.84\text{mg.L}^{-1}$ , com uma média de  $6.59\text{mg.L}^{-1}$  para o eixo Leste-Oeste; e  $19.37\text{mg.L}^{-1}$ ,  $5.44\text{mg.L}^{-1}$  e  $8.59\text{mg.L}^{-1}$  para o eixo Norte-Sul (valores máximo, mínimo e médio, respectivamente). Ao longo dos transectos de salinidade (em direção às desembocaduras do sistema estuarino), a concentração do carbono orgânico foi constante, enquanto a absorvância do CDOM diminuiu, inferindo na existência de diversas fontes de material orgânico para o sistema. As saturações do  $\text{CO}_2$  e  $\text{O}_2$  foram relacionadas com a salinidade e também se mostraram correlacionadas com a absorvância do CDOM nos comprimentos de onda de 320 e 443nm (61% e 47% para o  $\text{O}_2$ ; 63% e 46% para o  $\text{CO}_2$ , respectivamente). Os eixos Leste-Oeste e Norte-Sul exibiram médias de fluxo de difusão de  $1.74$  e  $2.72\text{mM.m}^{-2}.\text{h}^{-1}$ . As exportações de COD e COP na desembocadura Norte foi de  $21.39\text{kg.s}^{-1}$  e  $8.30\text{kg.s}^{-1}$ , respectivamente; enquanto para a desembocadura Sul, as médias foram de  $-1.57\text{kg.s}^{-1}$  (em direção ao estuário) e  $26.40\text{kg.s}^{-1}$ , respectivamente. A presença de substâncias húmicas no sistema afeta a produção primária, e conseqüentemente afeta as saturações de  $\text{CO}_2$  e  $\text{O}_2$ . O estuário demonstrou um metabolismo heterotrófico, exportando grandes quantidades de  $\text{CO}_2$  para a atmosfera e grandes quantidades de carbono orgânico, até mesmo quando comparado com alguns dos maiores rios do planeta.

## ABSTRACT

Variations of organic carbon sources and its spatial variations are important to comprehend the balances of the different organic carbon phases in the coastal zones. Surveys were made along the salinity gradients and mouths of the Paranaguá Estuarine Complex (PEC), objecting to analyze the spatial distribution of Particulate Organic Carbon (POC) and Dissolved Organic Carbon (DOC), variations of CO<sub>2</sub> and O<sub>2</sub> saturations, metabolic analysis of the estuary, the CO<sub>2</sub> diffusive fluxes and the POC and DOC exportations to the adjacent coastal waters of the PEC. The system is located in the Paraná State, south of Brazil, comprising 612km<sup>2</sup> and a water volume in the order of 2 x 10<sup>9</sup>m<sup>3</sup>. Samples were collected, during four sampling campaigns, along the salinity gradients in the two axes, North-South and East-West axes, and in the Northern and Southern Mouths of the system. The organic carbon samples were analyzed by HTC TOC-500 Shimadzu equipment; diffusive fluxes at the air-water interface were estimated according to Carmouze (1994) and the exportations were based on the anchoring of the S4 Current Meter, measuring currents and water discharge for an entire tidal cycle. The main results showed a variation of the organic carbon concentration values: maximum of 13.56mg.L<sup>-1</sup>, minimum of 3.84mg.L<sup>-1</sup> with a mean of 6.59mg.L<sup>-1</sup> for the East-West Axis; and 19.37mg.L<sup>-1</sup>, 5.44mg.L<sup>-1</sup> and 8.59mg.L<sup>-1</sup> for the North-South Axis (maximum, minimum and mean values, respectively). Along the salinity transects (direction to the mouth of the estuarine system), the absorbance of CDOM diminishes, which infer different sources of organic matter to the system. The saturations of CO<sub>2</sub> and O<sub>2</sub> were related with the salinity and also showed correlations with the absorbance of CDOM at 320 and 443nm (61% and 47% for O<sub>2</sub>; 63% and 46% for CO<sub>2</sub>, respectively). The East-West and North-South axes exhibited mean diffusive fluxes of 1.74 and 2.72mM.m<sup>-2</sup>.h<sup>-1</sup>. The exportations of DOC and POC at the Northern Mouth had an average flux of 21.39kg.s<sup>-1</sup> and 8.30kg.s<sup>-1</sup>, respectively; while the Southern mouth had an average flux of -1.57kg.s<sup>-1</sup> (towards the estuary) and 26.40kg.s<sup>-1</sup>, respectively. The presence of humic substances in the system affects the primary production, consequently affecting the CO<sub>2</sub> and O<sub>2</sub> saturations. The estuarine system reflects a heterotrophic metabolism, exporting high amounts of CO<sub>2</sub> to the atmosphere and high quantities of Organic Carbon to the adjacent ocean, even when compared to the major rivers in the world.

**PALAVRAS-CHAVE**

**Carbon, estuary, subtropical, fluxes, Brazil, alkalinity**

## LISTA DE FIGURAS

Figure 1: Paranaguá Estuarine Complex with the two main axes and the sampling sites.....	6
Figure 2: Variation in salinity and pH along the (a) East-West and (b) North-South axes of the Paranaguá Estuarine Complex. Figure 2a- sampling site 1 is the westernmost site; Figure 2b- sampling site 1 is the northernmost site.....	9
Figure 3: Dissolved oxygen and carbon dioxide saturation rates (%) along the sampling sites of the East-West and North-South axes of the Paranaguá Estuarine Complex (a and c); Figure 3a- sampling site 1 is the westernmost site; Figure 3c- sampling site 1 is the northernmost site. Figure 3b and 3d show correlations between dissolved oxygen and carbon dioxide saturation rates, with indication of the regression equation and $r^2$ .....	12
Figure 4: Total Organic Carbon (TOC; $\text{mg.L}^{-1}$ ; “4a” and “4c”) and Particulate Organic Carbon (POC; $\text{mg.L}^{-1}$ ; “4b” and “4d”) variations along the sampling sites of the East-West and North-South axes of the Paranaguá Estuarine Complex.....	13
Figure 5: Dissolved Organic Carbon (DOC; $\text{mg.L}^{-1}$ ) and light absorbance (320nm and 443nm) variations along the sampling sites of the East-West and North-South axes of the Paranaguá Estuarine Complex.....	14
Figure 6: Representativity of Dissolved Organic Carbon (DOC; %) and Particulate Organic Carbon (POC; %) in the Total Organic Carbon (TOC) along the sampling sites of the East-West and North-South axes of the Paranaguá Estuarine Complex.....	16
Figure 7: Correlation between salinity and alkalinity, with the respective linear model and $r^2$ , the p.value for the figure 8a is 0.09 and for the figure 8b is <0.01.....	17
Figure 8: PCA of variables collected for the East-West axis of the Paranaguá Estuarine Complex. The PCA demonstrated that 70.4% of the variance in the data was explained by the first and second principal component (50.66%- principal component 1; 19.74%- principal component 2).....	18
Figure 9: The PCA of the samples collected for the East-West axis of the Paranaguá Estuarine Complex was plotted with the squared cosine analysis to avoid interpretation of errors due to effects of the projection. Identification of the samples: “E-W_number of sample site”.....	19
Figure 10: PCA of variables collected for the North-South axis of the Paranaguá Estuarine Complex. The PCA demonstrated that 72.6% of the variance in the data was explained by the first and second principal component (59.2%-principal component 1; 13.4%- principal component 2).....	20
Figure 11: The PCA of the samples collected for the North-South axis of the Paranaguá Estuarine Complex was plotted with the squared cosine analysis to avoid interpretation of errors due to effects of the projection. Identification of the samples: “N-S_number of sample site”.....	21
Figure 12: Carbon dioxide ( $\text{CO}_2$ ; $\text{mM.m}^{-2}.\text{h}^{-1}$ ) diffusive flux variations along the sampling sites of the East-West and North-South axes of the Paranaguá Estuarine Complex.....	22

Figure 13: Velocity of the currents for the tidal cycle in the dimensionless depth at the Northern Mouth (figure 12a) - on 31/08/2012.....	23
Figure 14: Velocity of the currents for the tidal cycle in the dimensionless depth at the Southern Mouth of the Paranaguá Estuarine Complex (figure 12b) – on 02/09/2012.....	23

**TABLE'S LIST**

Table 1: a) Comparison of mean grain size distributions (%) and b) sorting distributions for the East-West and North-South axes of the Paranaguá Estuarine Complex: AG- coarse sand; AM- medium sand; AF- fine sand; AMF- very-fine sand; SG- coarse silt; SM- medium silt; SF- fine silt; MPS- very-poorly selected; PS- poorly selected; MS- moderate selected; BS- well selected; MBS- very-well selected. *Modified from Lamour <i>et al.</i> (2004).....	5
Table 2: Mean values of Dissolved Organic Carbon (DOC), Particulate Organic Carbon (POC), water discharge, fluxes of DOC and POC during the ebb and flood tide for the two mouths of the Paranaguá Estuarine Complex – negative and positive values of fluxes represent fluxes towards the estuary and towards the adjacent ocean, respectively.....	24
Table 3: Major worldwide riverine discharges ( $\text{m}^3 \cdot \text{s}^{-1}$ ), Dissolved and Particulate Organic fluxes ( $\text{kg} \cdot \text{s}^{-1}$ ) and global representativity of organic carbon input into the oceans.....	25

## CONTENT

<b>1</b> .....	<b>INTRODUCTION</b>
1.1.....	Objectives
1.2.....	Specific objectives
<b>2</b> .....	<b>MATERIAL AND METHODS</b>
2.1.....	Study area
2.1.1.....	Paranaguá Estuarine Complex
2.2.....	Gradient approach
2.3.....	Sample processing and laboratory analysis
2.4.....	Data analysis
2.5.....	Estimates of estuarine metabolism and diffusive carbon fluxes
2.6.....	Estimate of carbon export to the adjacent coastal zone
<b>3</b> .....	<b>RESULTS AND DISCUSSION</b>
3.1.....	Gradient approach
3.2.....	Estimates of estuarine metabolism and diffusive carbon fluxes
3.3.....	Estimate of carbon export to the adjacent coastal zone
<b>4</b> .....	<b>CONCLUSION</b>
<b>5</b> .....	<b>REFERENCES</b>
<b>6</b> .....	<b>APPENDIX</b>

## 1. INTRODUCTION

During its transport and biogeochemical cycling in coastal zones, carbon undergoes modifications and transformations due to human activities such as hydrological alterations for sanitation, sewage flows and increases of carbon dioxide emissions (REGNIER *et al.*, 2013; WOLLAST, 1993). A proper understanding of these modifications is extremely important to comprehend the global carbon cycles and global warming. Terrestrial organic matter is transported into coastal zones via two major routes, rivers and atmosphere (SEKI *et al.*, 2006). Hence, coastal zones and estuaries are important repositories of Total Organic Carbon (TOC) and play a key role in the global carbon cycle (SALIOT *et al.*, 2002).

In the marine environment, carbon can be found in organic or inorganic form. The inorganic fraction comprises particulate and dissolved forms; the organic fraction is found as particulate, dissolved and colloidal. Particulate Organic Carbon (POC) is transported to estuaries through a variety of allochthonous and autochthonous ways. These include riverine transport, marine plankton; bordering (e.g. mangrove, fresh/salt marshes and wetland systems); secondary production (e.g. fish, benthic animals); aquatic vegetation (e.g. seagrasses); estuarine plankton (e.g. benthic and epiphytic micro-macroalgae) (BIACHI & BAUER, 2011).

The Colloidal fraction of the Organic Carbon (COC) predominates in fresh (riverine) water (WHITEHOUSE *et al.*, 1989; BENNER & HEDGES, 1993), together with humic substances, also called yellow substances, Gelbstoff or CDOM (KALLE, 1938). This humic fraction contains highly complex structures and can contribute to 40% to 60% of the Dissolved Organic Carbon (DOC), and be responsible for up to 85% of the color of a water sample (SPITZY & ITTEKKOT, 1986). Humic substances can act as a pH buffer and show important interactions with metallic species (ROCHA & ROSA, 2003). It presents excitation and emission in spectra at highly variable range, usually between 300-400 nm and 400-500nm, respectively (BLOUGH & DEL VECCHIO, 2002; NELSON & SIEGEL, 2002). Therefore, some referenced parts of the light spectrum are defined, indicating the presence of heavy refractory carbon, i.e. humic substances.

The dissolved organic form is the predominant form of Organic Carbon (OC) in oceanic basins, and the secondmost important form in other marine environments (HANSELL & CARLSON, 1998b; HANSELL & CARLSON, 2002). Moreover, it is involved in several marine chemical processes, like the solubilization of hydrocarbons (BOEHM & QUINN, 1973), particulate matter formation (KROM & SHOLKOVITZ, 1997), interactions with iron and manganese minerals (GUO *et al.*, 1994; THIMSEN & KEIL, 1998), and as a reagent in marine photochemical reactions (KIEBER *et al.*, 1990). The DOC concentrations in coastal waters are highly correlated with terrigenous transport.

In extreme cases, such as in the northern part of the South China Sea, DOC may comprise up to 95% of the marine TOC (HUNG *et al.*, 2007), and 34% of the riverine TOC in the Mississippi River by Wang *et al.* (2004).

Williams & Druffel (1987) reported that the estimated fluxes of terrestrial DOC are sufficient to support the turnover of carbon in oceans. The low fluvial contribution of DOC to the pool of the marine dissolved organic matter (10%) is explained by the observation that 63 to 73% of the fluvial DOC in oceans is decomposed over time scales of years or decades (MEYERS-CHULTE & HEDGES, 1986; HEDGES *et al.*, 1997; HANSELL *et al.*, 2004). In estuaries, such DOC decomposition may result from mixture processes (HEDGES *et al.*, 1997; CAUWET, 2002), more specifically from the processes of flocculation and microbial degradation (CARLSON, 2002). In high-salinity environments, it occurs as result of photo-oxidation processes (BENNER & OPSAHL, 2001).

The OC is of great importance in the ocean-atmosphere interaction, because its decomposition regenerates nutrients into the environment and exports CO<sub>2</sub> to the atmosphere (BAUM *et al.*, 2007). In this context, correct estimates of OC concentration are important to understand the marine biogeochemical cycles of carbon (AMON & BENNER, 1994) and by extension the global carbon cycle (HEDGES, 1992).

The concentrations of Dissolved Inorganic Carbon (total CO<sub>2</sub> / DIC) in the ocean and atmosphere affect the climate and living conditions for many organisms. DIC concentrations in open oceans and its fluxes at the air-water interface have been fairly well studied; yet, DIC quantification at the land-ocean interface are less well understood and may fluctuate considerably among between years (CHEN *et al.*, 2013; KHATIWALA *et al.*, 2013; WANNINKHOF *et al.*, 2013).

In estuaries or enclosed water systems, the dynamics and variations of the carbonic forms can be higher than in the adjacent oceanic areas, due to the influence of the fluvial processes that tend to modify the salinity of these enclosed water systems, the presence of tidal currents, mangroves, reefs and seagrass beds associated with it and of anthropogenic actions. Therefore, understanding the variations on these carbonic forms and their metabolic activity in the pelagic compartments of these systems becomes extremely important.

### 1.1. Objectives

Evaluate the spatial behavior of quantitative and qualitative parameters in two salinity gradients in the Paranaguá Estuarine Complex (PEC) during an ebb spring tide, including Total Organic Carbon, Particulate Organic Carbon, Dissolved Organic Carbon, Dissolved Inorganic Carbon, Dissolved Oxygen and Hydrogenionic potential;

### 1.2. Specific objectives

- Estimates of diffusive fluxes of CO<sub>2</sub> in the ocean-atmosphere interface of the PEC;
- Estimate POC and DOC exportation from the PEC to the adjacent coastal waters.

## 2. MATERIAL AND METHODS

### 2.1. Study area

#### 2.1.1. Paranaguá Estuarine Complex

The Paranaguá Estuarine Complex (PEC) is located in the central-north coast of Paraná State in southern Brazil (Figure 1). It comprises an area of 612km<sup>2</sup> and an average water volume in the order of 2x10<sup>9</sup>m<sup>3</sup> (PAULA & CUNICO, 2007). According to Köppen the climate is classified as Cfa - always humid tropical rainy - which “C” means pluvial tropical weather, “f” means always humid with rains occurring in all months of the year; and “a” means the average air temperature during the warmest month of the year is always above 22°C (PAULA & CUNICO, 2007). Its drainage basin comprises an area of approximately 3754km<sup>2</sup>, which represents 65% of the drainage basin of the Paraná State Coastal Zone (PLANOS LOCAIS DE DESENVOLVIMENTO DA MARICULTURA: PARANÁ, 2010; LIBARDONI, unpublished monograph 2012). In the Coastal Plain, the annual mean air temperature is 21.1°C; along the contiguous Sea Mountain Chain the annual mean temperature is 14°C with a minimum of 7°C (PAULA & CUNICO, 2007). The average and maximum water depths of the estuarine complex are 5.4 and 33 meters, respectively. The tidal prism is 580 x 10<sup>6</sup> m<sup>3</sup> and the amplitude is 2.2 meters. The PEC is classified as a partially mixed estuary with a residence time of 3.5 days (MARONE *et al.*, 1995; MARONE *et al.*, 2005).

The study site comprises the two main axes of the PEC: a) Laranjeiras Bay, situated in the North-South Axis (N-S), which has a low population density of 2 inhabitants per km<sup>2</sup>, and b) Paranaguá and Antonina Bay, in the East-West Axis (E-W), where harbor activities are being developed as well as fisheries and tourism, and with a population density of 200 inhabitants per km<sup>2</sup> (MARONE *et al.*, 2005).

The PEC sediments differ in their mean grain size distributions, sorting, carbonate and organic content between the two estuarine axes (Table 1) (Lamour *et al.*, 2004). The carbonate content for the E-W varies between 5 and 20% from westernmost to the easternmost section, respectively; while the organic content appears to be related to the margin of the axis, since presents percentages of 0% at the center of the axis and between 15 to 35% at its borders; in the southern mouth of the PEC, the organic content varied between 0 and 5%. Carbonate content in sediments along the N-S axis are generally < 5%, and organic content varies between 0 and 15%, with its maximum in the northern mouth of the bay.

Table 1. **a)** Comparison of a) mean grain size distributions (%) and b) sorting distributions for the East-West and North-South axes of the Paranaguá Estuarine Complex: AG- coarse sand; AM- medium sand; AF- fine sand; AMF- very-fine sand; SG- coarse silt; SM- medium silt; SF- fine silt; MPS- very-poorly selected; PS- poorly selected; MS- moderate selected; BS- well selected; MBS- very-well selected. \*Modified from Lamour *et al.* (2004).

<b>a) Mean Grain Size (Phi)</b>	AG	A M	AF	A MF	S G	S M	S F
<i>Axes</i>	%	%	%	%	%	%	%
<i>East-West Axis</i>	3.1	6	29.	2	1	1	5.
<i>North-South Axis</i>	0.9	5	52.	1	1	6	4.
		.0	3	7.9	2.9	.5	3

<b>b) Sorting Distributions</b>	M PS	P S	M S	B S	M BS
<i>Axes</i>	%	%	%	%	%
<i>East-West Axis</i>	1	64	1	4	1.
<i>North-South Axis</i>	3.0	.2	7.0	.5	3
	3	59	7	1	-
	0.8	.6	.8	.8	

## 2.2. Gradient approach

The sampling sites were positioned in the navigation channels of the two principal axes (North-South and East-West) of the PEC. Sampling was performed during a low spring-tide condition with water samples collected along two transects, comprising 28 sampling sites along the East-West Axis and 25 along the North-South Axis. Each transect was sampled completely in a single day in July/2012 and August/2012, respectively. The locations of the sampling sites (Figure 1) were recorded with a GARMIN GPS (Hcx).

Samples of surficial water were collected with the aid of a Niskin Bottle (Niskin Sampling Bottle Model 1010-1.2 TO 30 L) and aliquots were taken to determine the dissolved oxygen (DO), alkalinity, pH, salinity, temperature, TOC, POC, DOC and CDOM absorbance, in two length spectra, at 320nm and 443nm.

Samples for OC analysis were stored in polyethylene bottles, pre-washed with diluted HCl (10%), and kept in the dark, in a thermal box filled with ice until analysis.

Samples for DO analysis were conditioned in glass bottles with polished cover and pre-determined volume; manganese chloride (1<sup>st</sup> reagent) and potassium iodide (2<sup>nd</sup> reagent) were added to fixate the Dissolved Oxygen. The samples were maintained in a thermal box to avoid changes in temperature and any effects of light on the oxygen level until arrival at the laboratory.

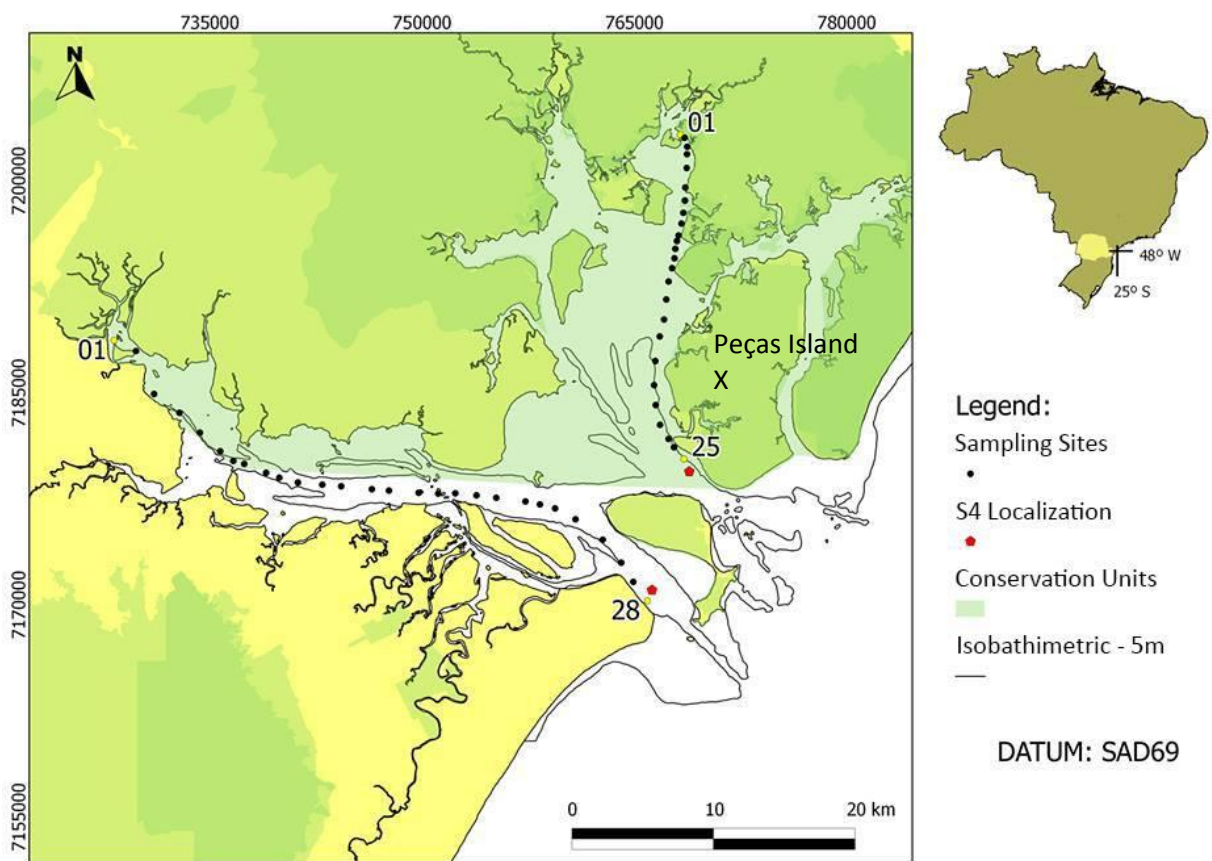


Figure 1: Paranaguá Estuarine Complex with the two main axes and the sampling sites.

The Hydrogenionic potential was measured in situ with a pH meter (HANNA instruments), temperature was measured in situ with a conventional thermometer and salinity with a hand refractometer (ATAGO).

Samples for alkalinity measurements were stored in polyethylene bottles (15mL of sample plus 0.5mL HCl 0.1N) and kept in the dark until further processing.

### 2.3. Sample processing and laboratory analysis

Dissolved Oxygen was analyzed by Winkler titration (1888), following GRASHOFF *et al.* (1983) immediately after arrival in the laboratory.

Alkalinity was determined through HCl titration (0.1N) and calculated using ALCAGRAN software (CARMOUZE, 1994).

In order to analyze the DOC and CDOM, 100mL-aliquots of each sample were filtered through 0.2 $\mu$ m Ester Mixture filters (FMAIA), pre-washed with Hydrochloric acid (5%) for 15 minutes. 20mL-aliquots of the filtered sample were analyzed with an UV spectrophotometer (Shimadzu) on a spectral range

of 800 to 250nm (nanometers) to obtain the CDOM absorbance. The samples used to determine TOC, DOC and POC fractions were preserved with Hydrochloric acid in a final concentration of 0.03%. Analysis of TOC and DOC were done by the High Temperature Combustion Method (HTC), on Shimadzu TOC-5000 analyzer. The POC was determined as the difference between TOC and DOC.

#### 2.4. Data analysis

The data was subjected to linear regressions and Principal Component Analysis (PCA) - made with the analyzed variables: salinity, temperature, pH, saturation of Dissolved Oxygen and CO<sub>2</sub>, TOC, POC and DOC concentrations, and the two light absorptions, in 320nm and 443nm by the Colored Dissolved Organic Matter, using R-Statistical Software (version 0.97.551). And auxiliary analysis and plots were made using the software Microsoft Excell 2010 and Surfer 11 for contouring, gridding and 3D surface mapping software.

#### 2.5. Estimates of estuarine metabolism and diffusive carbon fluxes

Following the protocol of CARMOUZE (1994), the metabolic activity (autotrophy/heterotrophy) of the PEC for the sampling period was established. This protocol emphasizes that the productions and eliminations of DO or O<sub>2</sub> and CO<sub>2</sub> by photosynthesis and respiration can be analyzed from the sum of all the inorganic carbon forms (Total Inorganic Carbon: ([H<sub>2</sub>CO<sub>3</sub>] + [HCO<sub>3</sub><sup>-</sup>] + [CO<sub>3</sub><sup>2-</sup>])). The variations on O<sub>2</sub> and CO<sub>2</sub> content, which are controlled by the biological processes and diffusive fluxes of these two gases, provide information to better understand the metabolic behavior of an ecosystem.

Estimates of the diffusive fluxes of CO<sub>2</sub> at the water-air interface also followed methodology adapted by CARMOUZE (1994). This approach considers the pH of the water at the water-air interface, together with alkalinity, temperature and wind intensity, to infer the volume of CO<sub>2</sub> in the environment and in equilibrium with the atmosphere ([CO<sub>2T</sub>]<sub>surface</sub> and [CO<sub>2T</sub>]<sub>equilibrium</sub>, respectively). Therefore, after the CO<sub>2</sub> analysis, the Fick's first law of diffusion was applied to calculate the diffusive flux of CO<sub>2</sub> (1):

$$(1) F_i = K_i \times \Delta[i] = K_i \times ([i]_{\text{equilibrium}} - [i]_{\text{surface}})$$

Where,  $F_i$  = Diffusive flux (mM.m<sup>-2</sup>.h<sup>-1</sup>)

$K_i$  = Coefficient of transference (m.h<sup>-1</sup>)

$\Delta[i]$  = Difference in the concentration of the species I (mM.m<sup>-3</sup>)

To estimate the diffusive flux of CO<sub>2</sub> along the tidal cycle in the two mouths of the PEC, an evaluation of the light period was made, considering the whole period of light, for the date when the survey was carried out at these specific regions (between 7:00 am and 7:00 pm). This analysis was made based on CARMOUZE (1994), considering the flux of gas at the water-air interface for a period of time as the product of the mean flux during this period and the Δt (duration of the period, in hours). The mean flux was calculated as an approximation of the semi-sum of the fluxes at the beginning and at the end of the period (2 and 3):

$$(2) \Delta(\text{CO}_{2\text{T}})_a = 0.5 \times (F_{\text{CO}_{2\text{T}} \text{ beginning}} + F_{\text{CO}_{2\text{T}} \text{ end}})$$

$$(3) \Delta(\text{CO}_{2\text{T}})_a = 0.5 \times ((K_{\text{CO}_{2\text{T}}} \times ([\text{CO}_{2\text{T}}]_{\text{equilibrium}} - [\text{CO}_{2\text{T}}]_{\text{surface}}))_b + (K_{\text{CO}_{2\text{T}}} \times ([\text{CO}_{2\text{T}}]_{\text{equilibrium}} - [\text{CO}_{2\text{T}}]_{\text{surface}}))_e) \times \Delta t$$

## 2.6. Estimate of carbon export to the adjacent coastal zone

To estimate the carbon export from the PEC to the adjacent coastal shelf, two anchoring of a S4 Current Meter were performed during a full spring tide cycle in the two mouths of the estuarine system, the Northern Mouth (N-M) on 31/08/2012 and the Southern Mouth (S-M) on 02/09/2012. Each anchoring lasted 13 hours, in which the following measurements were obtained: depth, water volume and velocity, direction and intensity of the currents. In addition, surface water samples were collected each hour to analyze the organic and inorganic dissolved carbon, dissolved oxygen, temperature, salinity, Hydrogenionic potential and alkalinity as detailed above. The resultant of the fluxes was calculated by the weighted arithmetic mean of the mean velocities and mean TOC, POC and DOC concentration for the period of ebb tide and the mean values for the period of flood tide.

### 3. RESULTS AND DISCUSSION

#### 3.1. Gradient approach

There was little or no temperature variation (17°C) along the East-West Axis of the PEC. Salinity varied between 15 and 30, and pH variation largely followed the salinity, increasing from 7.37 to 8.05 from west to east (Figure 2a). The lowest pH value was found at the intermediate site 11, which could be related to the Maximum Turbidity Zone of the estuary, since an abrupt change in color of the surface water has been observed here (NOERNBERG, 2001). This is further supported by the much higher CO<sub>2</sub> saturation at this site (Figure 3a), which likely reflects changes in primary production and controls the saturation of O<sub>2</sub> and CO<sub>2</sub> in the water (HERMAN & HEIP, 1999) resulting from a drop in light availability. There was also a drop in pH (7.88) in the easternmost site.

The transect along the North-South Axis of the PEC showed surface water temperatures of 19°C in the inner part of the system (sampling sites 1-20), decreasing slightly towards 18°C at the outer part of the bay (sampling sites 24 and 25). The salinity varied between 20 and 30 and the pH between 7.44 and 7.90. Both salinity and pH increased from North to South (Figure 2b). The relatively low pH at sites 21 and 22 (Figure 2b), possibly resulted from the influence of the delta of the Rio das Peças (Peças River), which originates from the Ilha das Peças (Peças Island, figure 1).

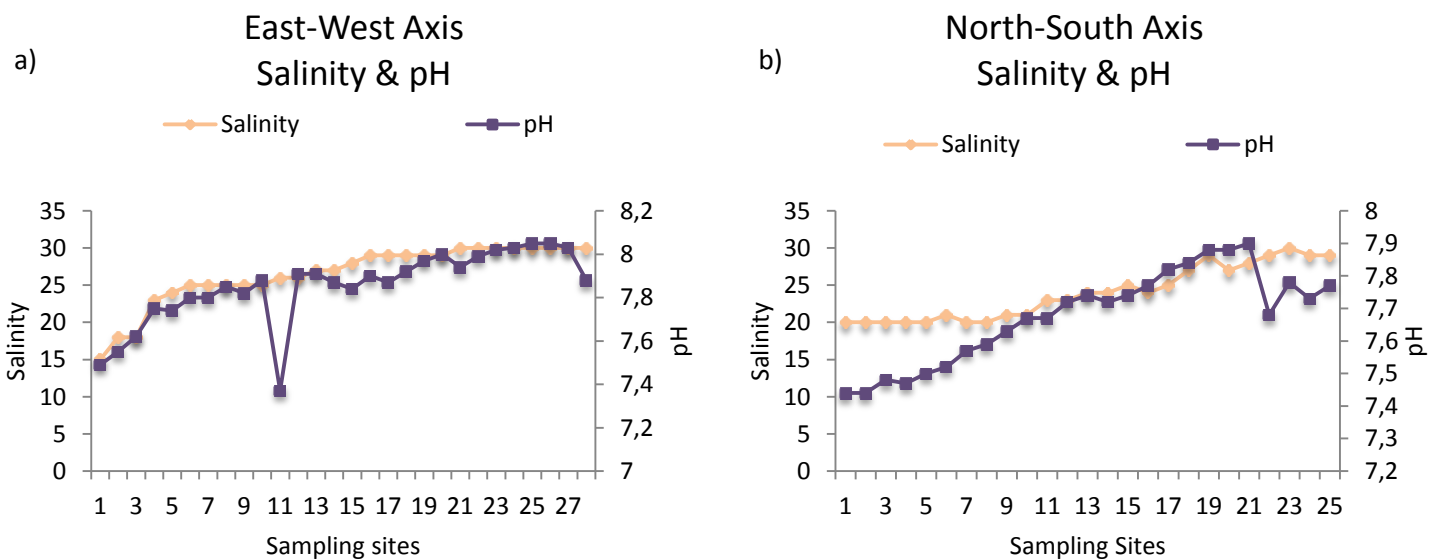


Figure 2. Variation in salinity and pH along the (a) East-West and (b) North-South axes of the Paranaguá Estuarine Complex. Figure 2a- sampling site 1 is the westernmost site; Figure 2b- sampling site 1 is the northernmost site.

O<sub>2</sub> saturation values increased slightly from West to East and exhibited significant positive correlation with salinity ( $r^2=0.48$ ,  $p<0.001$ ). By contrast, an inverse pattern was observed for CO<sub>2</sub> saturation, with values between 421%

and 128% at westernmost and easternmost site, respectively, decreasing significantly with increasing salinity ( $r^2=0.22$ ,  $p=0.007$ ). Inverse relations of  $\text{CO}_2$  and  $\text{O}_2$  and of  $\text{CO}_2$  and salinity were also found by Zhai & Dai (2009) in Changjiang Estuary, and by Bozec *et al.* (2012) in the Loire Estuary. They may be related to the marine water influence along the transect, together with the dominance of autotrophic organisms in these marine waters, diluting the terrestrial organic material increasing light penetration, allowing photosynthesis. A peak of  $\text{CO}_2$  at sampling site 11 coincided with the pH minimum and it is probably due to the MTZ, which can affect the fate and behavior of the organic matter.

Along the N-S,  $\text{O}_2$  saturation values increased towards the south, varying between 71% and 86% (sampling sites 1 to 25, respectively) and correlated positively with salinity ( $r^2=0.58$  and  $p<0.001$ ; Figure 3c).  $\text{CO}_2$  saturation values decreased from 304% to 139% at sites 1 and 25, respectively, with a strong inverse relationship with salinity ( $r^2=0.69$ ,  $p<0.001$ ).  $\text{CO}_2$  saturation rates in excess of 100% have also been observed for another tropical/subtropical surrounded by mangrove forests, Piaui River Estuary (SOUZA & COUTO, 1999) (values between 130 and 464%).

Mean TOC and POC concentrations were  $13.53\text{mg.L}^{-1}$  and  $6.77\text{mg.L}^{-1}$ , for the E-W respectively; and for the N-S, means of  $23.33\text{mg.L}^{-1}$  for TOC and  $5.63\text{mg.L}^{-1}$  for POC. Neither axes of PEC showed clear gradients along the transects (Figure 4).

These mean TOC and POC concentrations are higher than those concentrations observed for major rivers, as the Pearl River Delta (TOC= $4.30\text{mg.L}^{-1}$  and POC= $2.20\text{mg.L}^{-1}$ , HONG-GANG *et al.*, 2008), the Apure River (TOC= $5.20\text{mg.L}^{-1}$  and POC= $1.33\text{mg.L}^{-1}$ ), the Caura River, (TOC= $4.01\text{mg.L}^{-1}$  and POC= $0.77\text{mg.L}^{-1}$ ), the Orinoco River (TOC= $3.82\text{mg.L}^{-1}$  and POC= $0.91\text{mg.L}^{-1}$ , MORA *et al.*, 2014) and the Solimões River (POC= $1.19\text{mg.L}^{-1}$ , MOREIRA-TURCQ *et al.*, 2003). These first assessment and comparisons may indicate an incomplete and underestimate assessment of carbon dynamics in the coastal zone of southern Brazil.

Dissolved Organic Carbon concentrations showed marked variations (Figure 5a and 5c, respectively), along the E-W; ranging between  $3.84$  and  $13.56\text{mg.L}^{-1}$  with a mean of  $6.59\text{mg.L}^{-1}$ . DOC concentrations in the N-S varied from  $4.16$  to  $19.37\text{mg.L}^{-1}$  (mean of  $8.59\text{mg.L}^{-1}$ ). The diminishing of light absorbance with increasing salinity for both axes (Figures 5b and 5d) can be explained by the higher influence of less turbid marine water in the external part of the estuary (increasing salinity), meaning that the refractory part of the dissolved organic carbon is transported to the marine system by rivers (HARVEY & BORAN, 1985).

The mean DOC concentrations for both axes in the PEC are high when compared with those reported for the Pearl River Estuary ( $2.71\text{mg.L}^{-1}$ , HE *et al.*, 2010), the Middle Atlantic bay ( $1.32\text{mg.L}^{-1}$ , VODACEK *et al.*, 1997), the South Baltic Sea ( $6.54\text{mg.L}^{-1}$ , FERRARI *et al.*, 1996; FERRARI & DOWELL, 1998),

the Wanquan River (around  $2\text{mg.L}^{-1}$ , WU *et al.*, 2012) and the Schelde Estuary ( $4.6\text{mg.L}^{-1}$ , MUYLAERT *et al.*, 2005). However, they are low when compared to some boreal estuaries as the Karjaanjoki, and the Kiiminkijoki rivers ( $17.58\text{mg.L}^{-1}$ ,  $16.33\text{mg.L}^{-1}$ , respectively; ASMALA *et al.*, 2012). The DOC concentrations are also compared to those found in the morphoclimatic zones of higher concentration of DOC, as Taiga with typical concentrations of  $7\text{mg.L}^{-1}$  and Wet tropic (typical concentrations of  $8\text{mg.L}^{-1}$ ; CAUWET, 2002).

The Student's tests (t.test)\*, performed to observe if there were significant differences between the TOC, POC and DOC from the East-West and North-South axes showed that the only non-significant p.value was originated from the "TOC t.test" ( $p > 0.25$ ), which indicates that the concentration of total organic carbon observed for the two axes has no significant differences. On the contrary, the POC and DOC tests showed significant differences (POC t.test:  $p < 0.05$ ; DOC t.test:  $p < 0.05$ ). These results confirm the existing differences in the mean concentration values between POC and DOC for the N-S and E-W.

*\*The tests were performed only between each specific form – TOC from East-West Axis together with TOC from North-South Axis, POC from East-West Axis together with POC from North-South Axis and DOC from East-West Axis together with DOC from North-South Axis.*

The figure 6 shows the representativity of Particulate Organic Carbon and Dissolved Organic Carbon in the Total Organic Carbon for the sampling sites along the E-W and N-S axes. For the E-W, a mean of 52% is represented by the particulate fraction of carbon (POC), which is the opposite situation for the N-S, whereas a mean of 60% of the TOC is represented by the dissolved fraction of carbon (DOC).

Comparing the observed percentages of POC and DOC in the TOC for the E-W and N-S with other riverine systems, the PEC showed to behave differently than Apure, Caura and Orinoco rivers, in which 72, 82 and 78% of its TOC was found in the dissolved phase of the organic carbon (MORA *et al.*, 2014). However, for these rivers the POC percentage presented a high temporal and spatial variability, ranging between 1 and 45% (summer and fall, respectively). The highest percentage found in the Orinoco River (45% of POC) is comparable to the 40% found for the N-S.

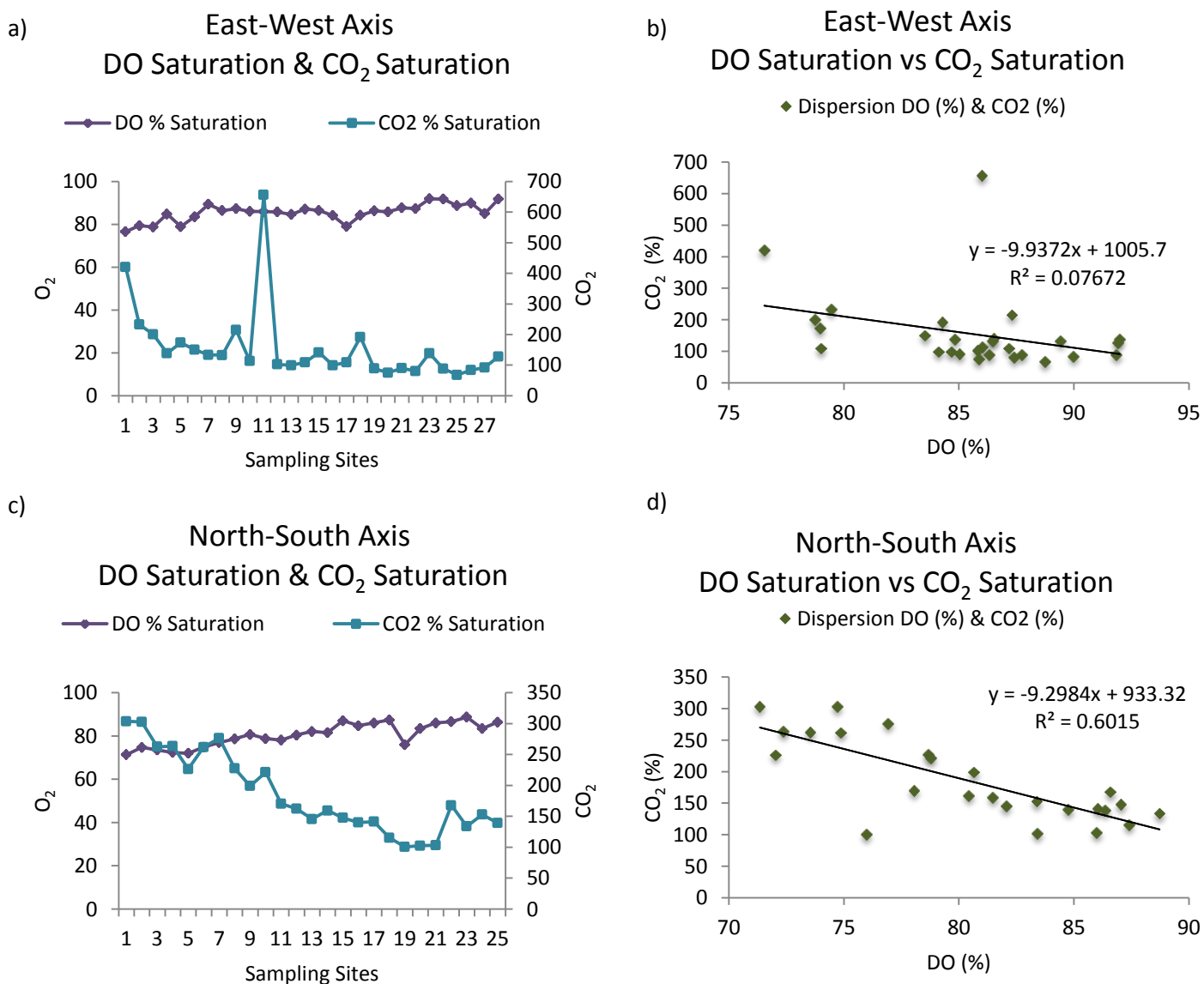


Figure 3. Dissolved oxygen and carbon dioxide saturation rates (%) along the sampling sites of the East-West and North-South axes of the Paranaguá Estuarine Complex (a and c). Figure 3a- sampling site 1 is the westernmost site; Figure 3c- sampling site 1 is the northernmost site. Figure 3b and 3d show correlations between dissolved oxygen and carbon dioxide saturation rates, with indication of the regression equation and  $r^2$ .

The tendency lines were plotted together with the variations of TOC, POC and DOC, to observe if the organic carbon phases tend to increase, decrease or maintain their concentrations showed differences for the two axes: The N-S showed a tendency of decreasing the TOC, POC and DOC concentrations, contrasting with the observed tendency of increasing TOC and DOC concentrations for the E-W (POC showed tendency of decreasing its concentration). These tendencies illustrate that for the E-W, the marine water,

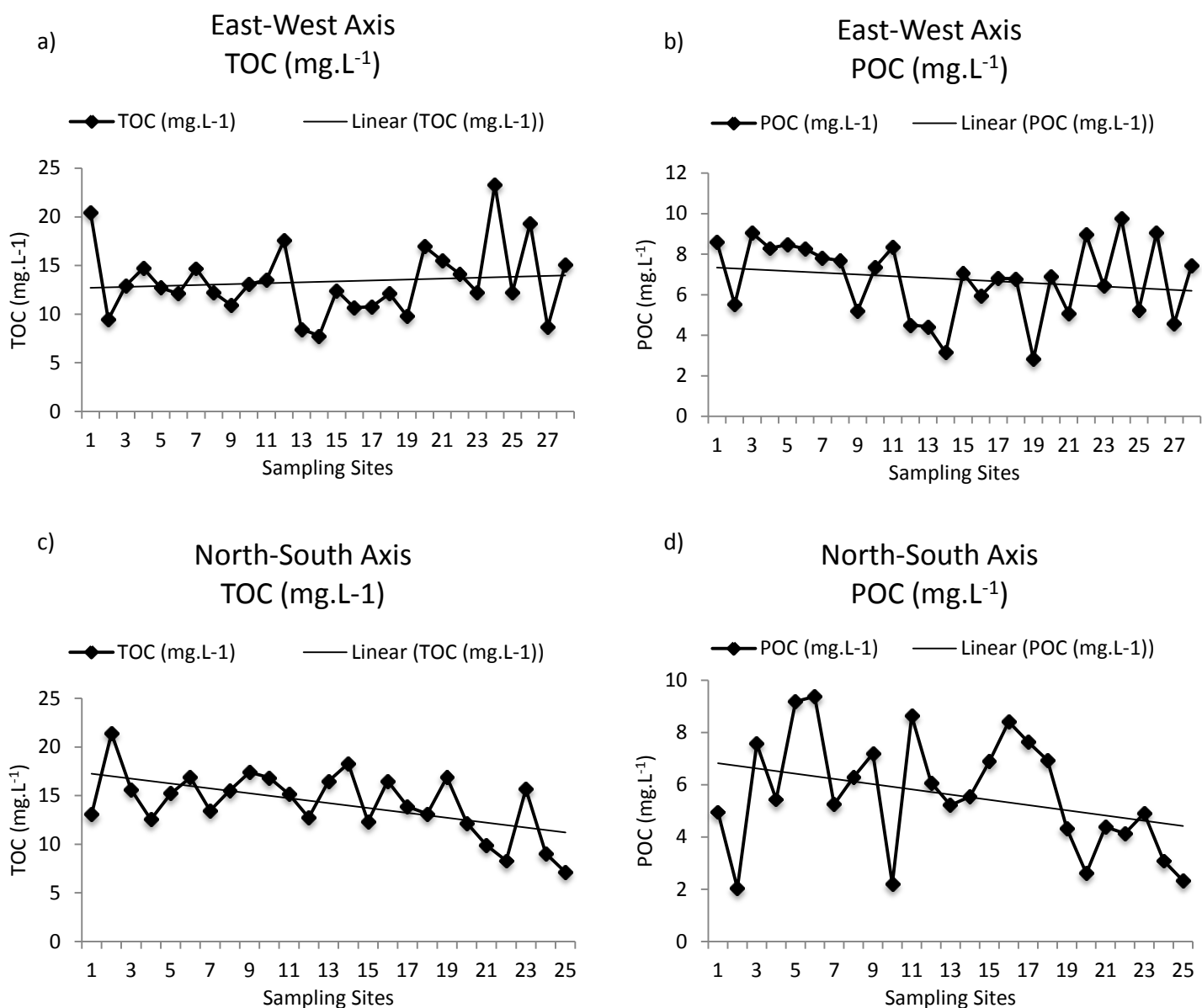


Figure 4. Total Organic Carbon (TOC; mg.L<sup>-1</sup>; “4a”) and “4c”) and Particulate Organic Carbon (POC; mg.L<sup>-1</sup>; “4b”) and “4d”) variations along the sampling sites of the East-West and North-South axes of the Paranaguá Estuarine Complex.

more present in the external part of the axis, might play a role on the concentration of organic carbon in the system. The system showed that the same amount of organic carbon is available for E-W and N-S, although, differential processes might be happening that determine which fraction of organic carbon will be more available and for which section of the system. Factors like differential production/exportation of POC and DOC by mangroves and/or riverine systems and/or primary producers to the PEC; and differential degradation/sequestration of POC and DOC by physic-biological processes might be affecting the percentage in which each phase is representing in each

section of the PEC. Apart of these possible situations, it was observed that the N-S contains more DOC than POC, and the contrary happens to the E-W.

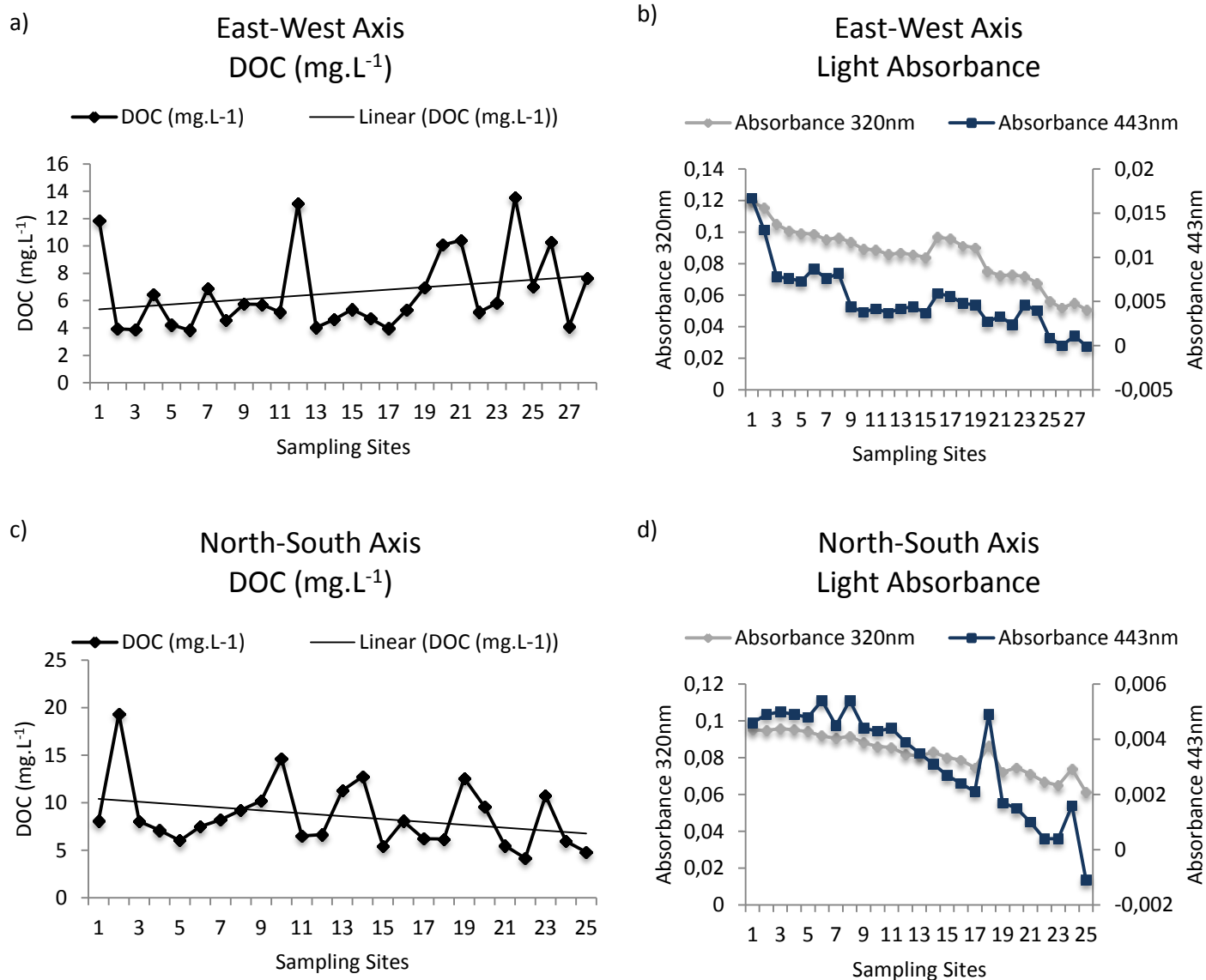


Figure 5. Dissolved Organic Carbon (DOC; mg.L<sup>-1</sup>) and light absorbance (320nm and 443nm) variations along the sampling sites of the East-West and North-South axes of the Paranaguá Estuarine Complex.

The PEC is known to shift conditions in fortnight and seasonal bases, and its stratification and mixing processes are highly dependent on tidal currents and freshwater discharge (Mantovanelli, *et al.*, 2004), which could explain the variation on the OC phases. DOC concentrations along the salinity gradient can be also related to two other important issues: the high number and diverse sources of inputs of organic matter, and the high number of very dynamic

removal processes of organic matter from the PEC system. The PEC has a drainage system with more than nine thousand water streams (ANGULO, 1992b) with eight major rivers, which show different fluxes of DOC, according to the seasonality (LIBARDONI, unpublished monograph 2012). Moreover, the surrounding area of the estuarine complex is dominated by mangrove systems (ANGULO, 1992b). Associated to these different sources of DOC (mangrove and river fluxes), several other mechanisms are responsible for Dissolved Organic Matter production in the ocean: phytoplankton extracellular release; grazer-mediated release and excretion; viral and bacterial cell lysis; solubilization of particles; and bacterial transformation and release (CAUWET, 2002). The removal processes can be separated into Biotic Consumption, including the demands from prokaryotic (Bacterial Growth Efficiency and Bacterial Carbon Demand) and eukaryotic (requiring organic molecules to meet their metabolic needs) organisms; and Abiotic Removal Processes, relating to adsorption and desorption, flocculation and deflocculation, aggregation, phototransformation by UV excitation and coagulation from seawater (CAUWET, 2002; JEONG *et al.*, 2014). The photochemical and microbial degradation, are often evaluated by analyzing the deviations from the conservative mixing (along salinity gradient; BORGES & ABRIL, 2012; BOWERS *et al.*, 2004; STEDMON & MARKAGER, 2003).

If the POC and DOC are behaving conservatively, it is expected a perfect relationship between them and salinity (BOWERS *et al.*, 2004). Therefore, the oscillation of both POC and DOC and also in alkalinity characterizes a non-conservative behavior of the organic matter while mixing with salinity. This contradicts some authors that have observed a conservative behavior along the salinity gradient (ALVAREZ-SALGADO & MILLER, 1998; MANTOURA & WOODWARD, 1983), but it is also sustained by Asmala *et al.* (2012), Borges & Abril (2012), Wang *et al.* (2004) and Sharp *et al.* (1984) who showed that the conservative or non-conservative behavior could be related to seasonality.

The variation on the linear regression of salinity and alkalinity (Figure 7) shows that for both axes, more specifically for the E-W (lower determination coefficient,  $r^2=0.10$ ), a diversity of sources of organic matter is being transported to the system. These non-conservative variations of alkalinity and salinity could also indicate anthropogenic source of OC to the system, therefore, affecting the estuary in terms of CO<sub>2</sub> emissions (BORGES & ABRIL, 2012; ABRIL, G. & FRANKIGNOULLE, 2000).

The PCA analysis for the E-W (Figure 8) shows a correlation between salinity and pH and the two light absorption coefficients, which could indicate a higher concentration of humic substances (CDOM) in the water, since the DOC of terrestrial origin is composed largely of humic and fulvic acids (HARVEY & BORAN, 1985). The PCA of the variables also confirms that the saturation of DO is correlated to the salinity and that the saturation of CO<sub>2</sub> has an inverse correlation with the salinity. The inverse relationship between DO saturation and the two light absorbance coefficients can be explained by the presence of the

humic substances in the water samples, leading to a change of the water color, which in turn controls the penetration and propagation of the solar radiation and therefore the primary production (NELSON & SIEGEL, 2002). The non-relation of the [TOC], [POC] and [DOC] with the other variables is explained by the high variation of OC sources, showing that for an accurate analysis and interpretation of the OC variation in the East-West Axis, organic matter composition analysis (High Resolution Mass Spectrometry) is necessary to better comprehend the effect of the water mixing in the different forms of TOC presented in the estuary.

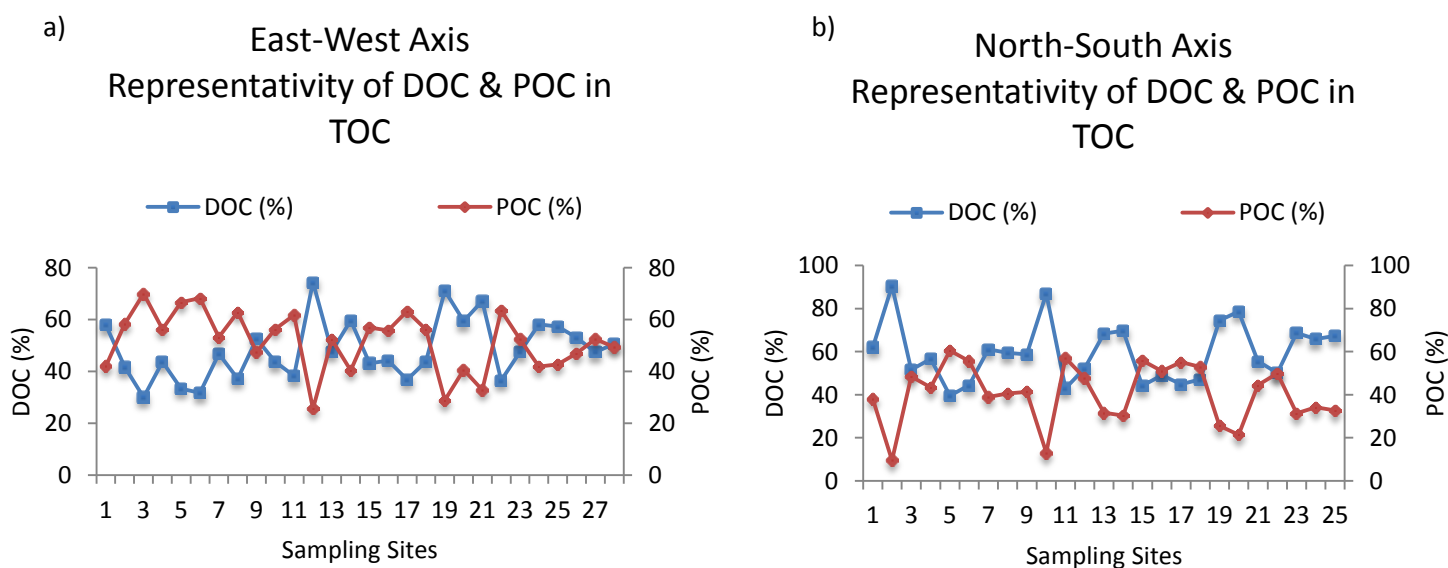


Figure 6. Representativity of Dissolved Organic Carbon (DOC; %) and Particulate Organic Carbon (POC; %) in the Total Organic Carbon (TOC) along the sampling sites of the East-West and North-South axes of the Paranaguá Estuarine Complex

Figure 9 is the PCA with the samples from the E-W. The squared cosine ( $\cos^2$ ) is used to indicate if the sample position can be confidently interpreted or not (LEGENDRE & LEGENDRE, 2012). In the present work, it was not interpreted when  $\cos^2$  was lower than 0.5. The analysis showed that it is possible to interpret the data based on the saturation of Dissolved Oxygen data - the samples were directly or inversely related to it. The first sample site and the sample site 11, in the inner part and in the TMZ of the E-W, respectively, are related to the high saturation of  $\text{CO}_2$  (420% and 657%) while the external sample sites of the estuary are inversely related to  $\text{CO}_2$  and positively related to  $\text{O}_2$ .

For the N-S, the PCA analysis (Figure 10) confirmed the positive and the inverse correlation of the salinity with DO and  $\text{CO}_2$ , respectively. It also indicates a positive relationship between OC (TOC, POC and DOC) and temperature. However, the latter was not confirmed by the regression of the

DOC concentration and temperature ( $r^2=0.08$ ,  $p=0.08$ ). The coefficient of light absorbance at 320nm and at 443nm appears to be positively correlated to the  $\text{CO}_2$  saturation, which is confirmed by the linear regressions (saturation  $\text{CO}_2$  and absorbance 320nm,  $r^2=0.63$  and  $p<0.001$ ; and saturation of  $\text{CO}_2$  and absorbance at 443nm,  $r^2=0.46$  and  $p<0.001$ ); and negatively with the saturation of DO (saturation of DO and absorbance at 320nm,  $r^2=0.61$  and  $p<0.001$ ; saturation of DO and absorbance at 443nm,  $r^2=0.47$  and  $p<0.001$ ). These correlations were also observed by Else *et al.* (2008), in which found negative correlation of  $\text{CO}_2$  with salinity and positive correlation with absorbance of CDOM (Pearson's  $r$  Correlation Coefficient equal to  $-0.79$  and  $0.72$ , respectively).

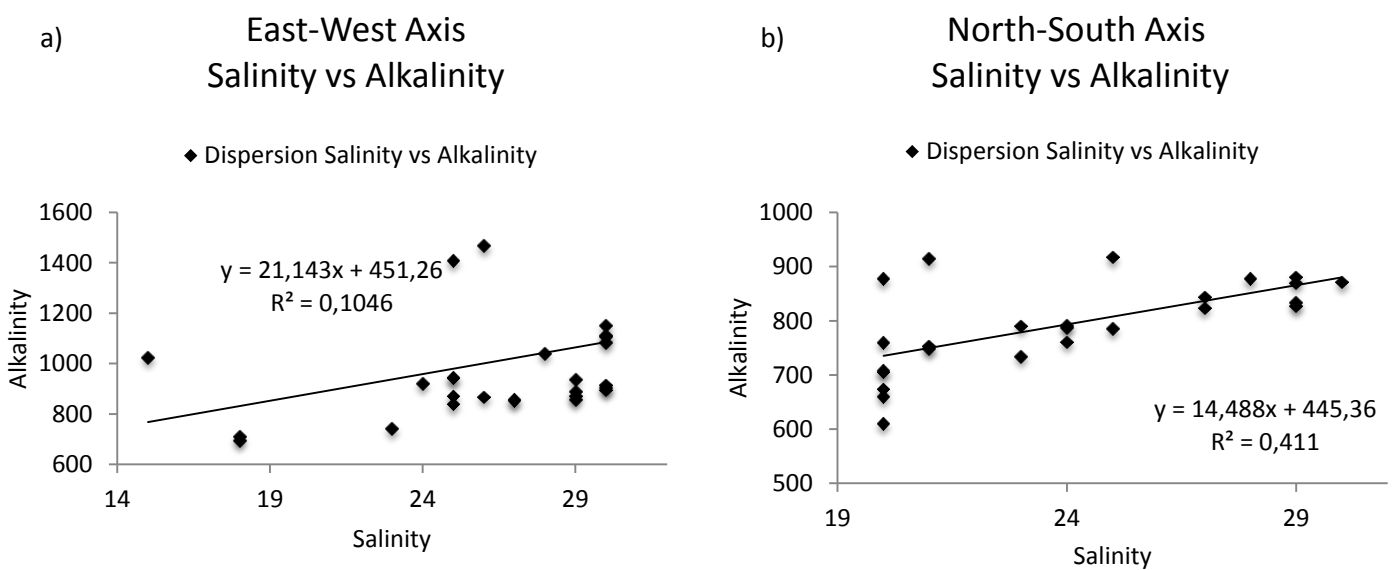


Figure 7. Correlation between salinity and alkalinity, with the respective linear model and  $r^2$ , the  $p$ .value for the figure 8a is 0.09 and for the figure 8b is  $<0.01$ .

The PCA for the samples was again plotted together with the squared cosine (Figure 11), and it is possible to see that samples from the inner part of the estuary (sample sites 1 to 8) are related to the saturation of  $\text{CO}_2$  and the external samples appears to be related to the saturation of DO (samples sites 20 to 25).

### 3.2. Estimates of estuarine metabolism and diffusive carbon fluxes

Based on the spatial variation of the Carbon Dioxide and Dissolved Oxygen saturation rates (Figure 3a and 3c) along the two main axes of the PEC and during the light period of the day, it was observed that for the E-W, the  $\text{CO}_2$  showed a saturation rate higher than 100% in 65% of the samples, with saturation rates two times higher than the equilibrium in 15% of the samples;

the mean of saturation for the East-West system was 155.4%. The O<sub>2</sub> did not present any saturation rate higher than 100% for the respective axis of the PEC, and the mean value was 85.56%. It was observed that for the N-S, the saturation rates of CO<sub>2</sub> were higher than 100% for all the analyzed sampling sites (mean=185.1%), and the O<sub>2</sub> saturation did not show values higher than 90% for any sample (mean=80.46%).

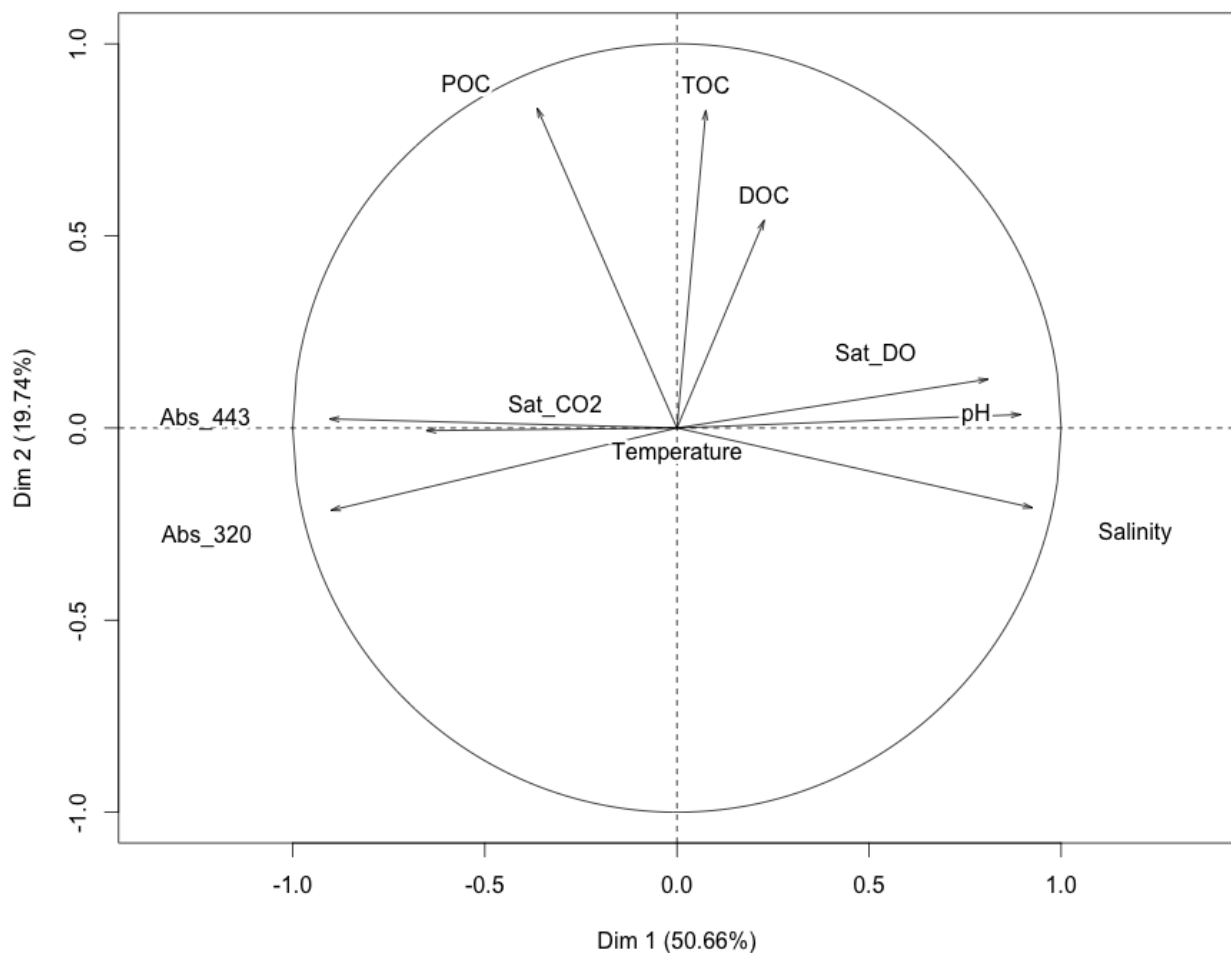


Figure 8. PCA of variables collected for the East-West axis of the Paranaguá Estuarine Complex. The PCA demonstrated that 70.4% of the variance in the data was explained by the first and second principal component (50.66%- principal component 1; 19.74%- principal component 2).

The analysis of the variation of metabolic rates for the environment provides information that supports a heterotrophic metabolism, for both axes of the PEC, which leads to a net export of CO<sub>2</sub> from the PEC to the atmosphere (Figure 12), which is a common situation for estuaries since river, salt marshes, mangroves and groundwater discharge increases CO<sub>2</sub> pressure by exporting carbon to estuaries (CHEN *et al.*, 2013). An average of 1.74mM.m<sup>-2</sup>.h<sup>-1</sup> and 2.72mM.m<sup>-2</sup>.h<sup>-1</sup> is being transported towards the air along the E-W and N-S, respectively.

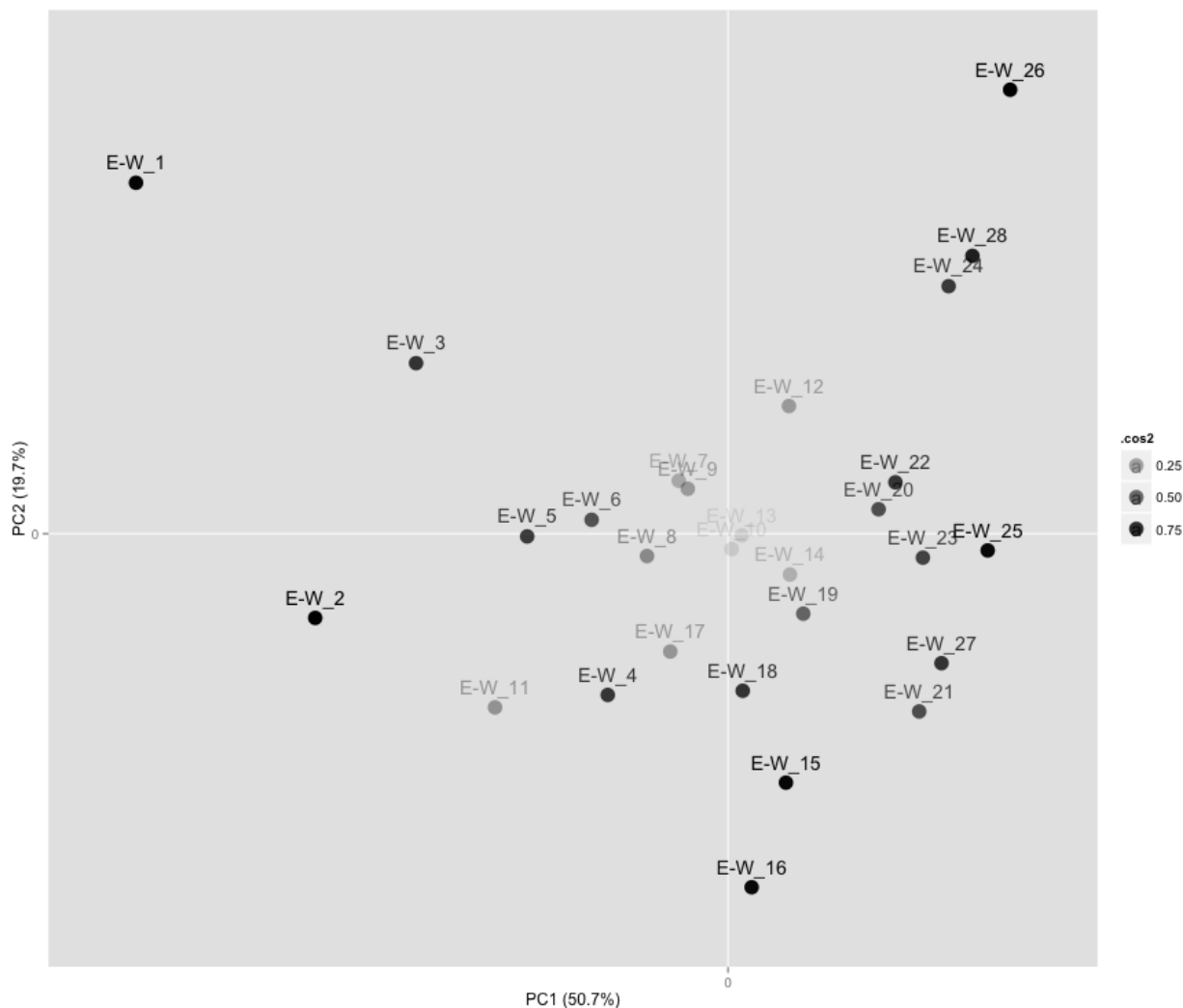


Figure 9. The PCA of the samples collected for the East-West axis of the Paranaguá Estuarine Complex was plotted with the squared cosine analysis to avoid interpretation of errors due to effects of the projection. Identification of the samples: “E-W\_number of sample site”.

A contrary situation was observed in the easternmost section of the E-W (sampling sites 19, 20, 21, 22, 24, 25, 26 and 27), which showed negative values of diffusive flux, representing a transport of  $\text{CO}_2$  from the air towards the water. The same situation was also observed for the both northern and southern mouths of the system, whereas for the whole sampling period, averages of  $10.68\text{mM}\cdot\text{m}^{-2}\cdot\text{h}^{-1}$  and  $4.73\text{mM}\cdot\text{m}^{-2}\cdot\text{h}^{-1}$  of  $\text{CO}_2$  were observed to be imported from the atmosphere in the S-M and N-M, respectively. This behavior of the PEC is sustained to Cai (2011), which summarizes that marsh-estuarine systems must be a sink of atmospheric  $\text{CO}_2$ , although the low-salinity locations in the estuary may have higher  $\text{CO}_2$  pressure than the atmosphere, releasing the  $\text{CO}_2$  (WANG & CAI, 2004). Chen & Borges (2009) citing Keil *et al.* (1997) support this argument, saying that 70% of the POC can be degraded in the estuary, providing the inorganic carbon to the system. For instance, Cai (2011)

suggests that the CO<sub>2</sub> loss from the estuaries, in general, “...is supported largely by microbial decomposition of OC in coastal wetlands”.

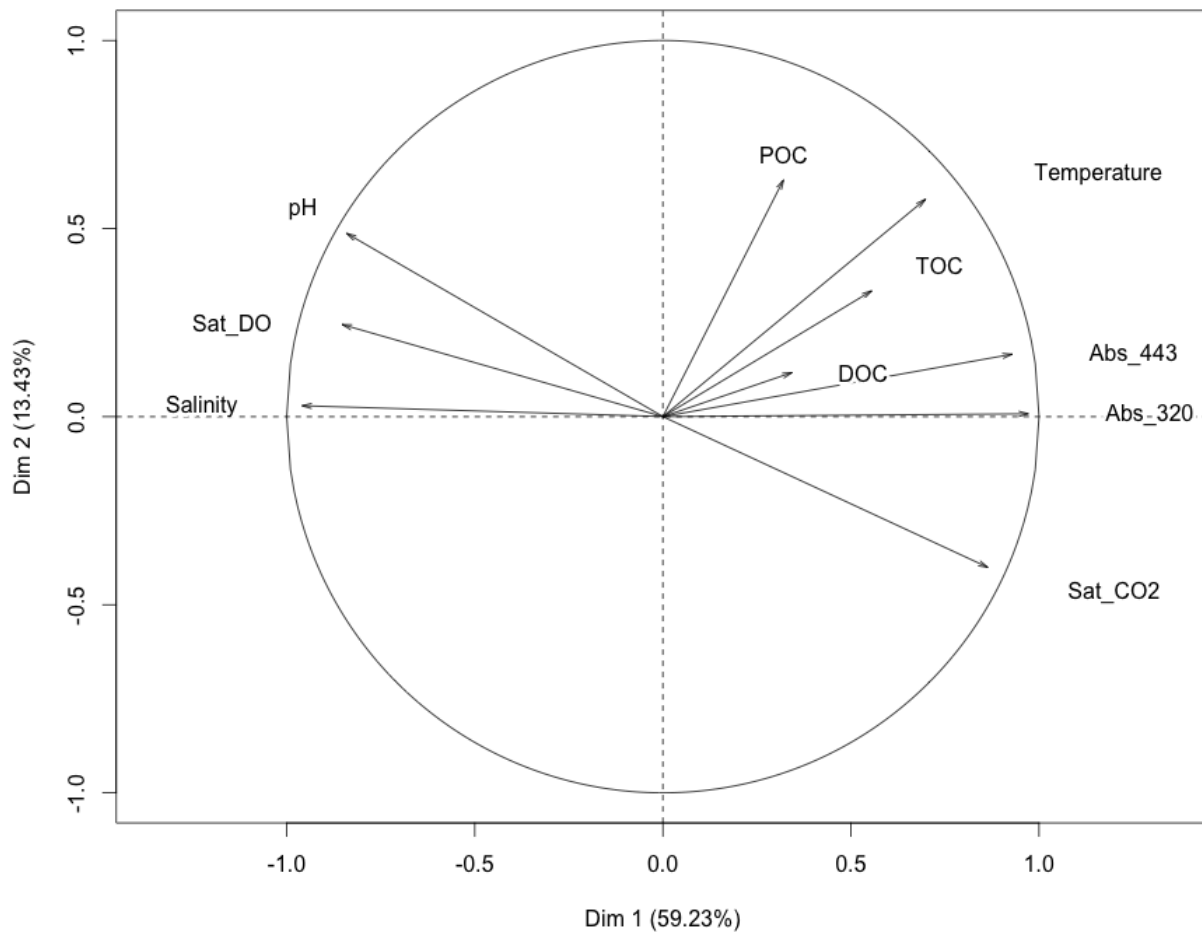


Figure 10. PCA of variables collected for the North-South axis of the Paranaguá Estuarine Complex. The PCA demonstrated that 72.6% of the variance in the data was explained by the first and second principal component (59.2%-principal component 1; 13.4%- principal component 2).

The diffusive fluxes of CO<sub>2</sub> were also calculated over a time basis, during 13 hours (light period), for both mouths of the system (N-M and S-M) using the adapted formula (3), taking into account that the wind velocity was below 5m.s<sup>-1</sup> for the entire sampling period. BOZEC *et al.* (2012) found that the CO<sub>2</sub> saturation pressure is highly dependent on, and controlled by, wind velocities, which led to an increase of approximately 4 times (185mM.m<sup>-2</sup>.d<sup>-1</sup>) in comparison to the annual mean flux (45mM.m<sup>-2</sup>.d<sup>-1</sup>) during the higher wind velocities for the region. The diffusive flux (towards the water) was -54.18mM.m<sup>-2</sup> for the N-M, and the mean CO<sub>2</sub> flux was -5.11mM.m<sup>-2</sup>.h<sup>-1</sup>; The S-M showed a flux of -75.48mM.m<sup>-2</sup> for the 13 hours and a mean of -10.68mM.m<sup>-2</sup>.h<sup>-1</sup>. Both analysis of metabolic rates and diffusive fluxes showed autotrophic behavior for the mouths of the PEC.

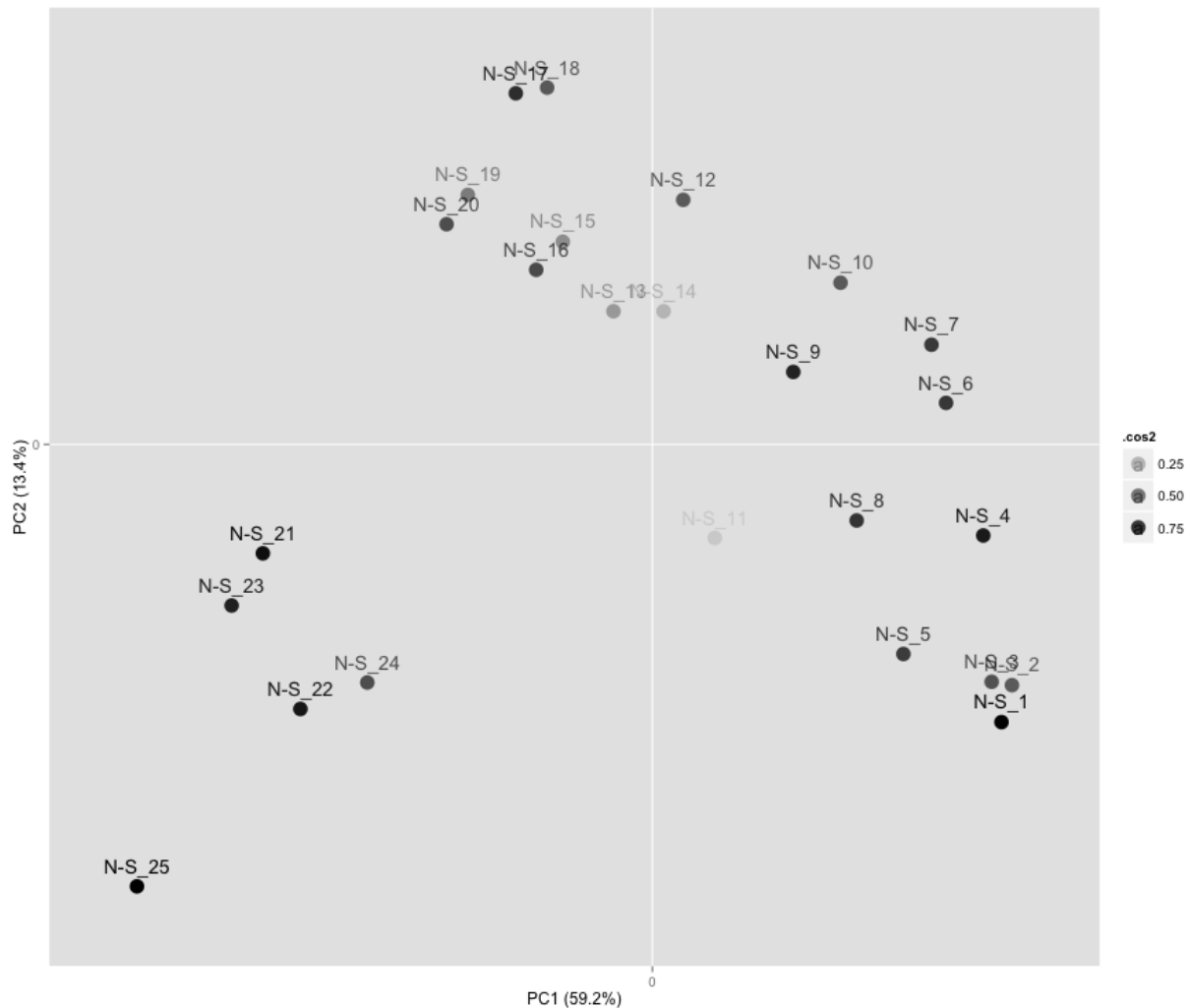


Figure 11. The PCA of the samples collected for the North-South axis of the Paranaguá Estuarine Complex was plotted with the squared cosine analysis to avoid interpretation of errors due to effects of the projection. Identification of the samples: “N-S\_number of sample site”.

The observed fluxes are high when compared to the 21 estuaries of the world that import  $\text{CO}_2$  from the atmosphere out of the 165 compiled by Chen *et al.* (2013). Although, the mean diffusive fluxes observed for the E-W and N-S showed to be higher than 90 worldwide estuaries that export  $\text{CO}_2$  to the atmosphere (CHEN *et al.*, 2013). It is important to emphasize that the referenced methodology was developed during the light period, which allows primary producers (if present in the environment) to incorporate  $\text{CO}_2$  to produce energy. Therefore, these values might be underestimated and a mean flux in which includes dark (night) period could show higher values of diffusive fluxes towards the atmosphere. And also that there are a variety of methods in the scientific community to estimate  $\text{CO}_2$  diffusive fluxes and to evaluate the

metabolism of a system. Therefore, it is important to establish a standard methodology to better estimate and compare CO<sub>2</sub> fluxes in the coastal zones.

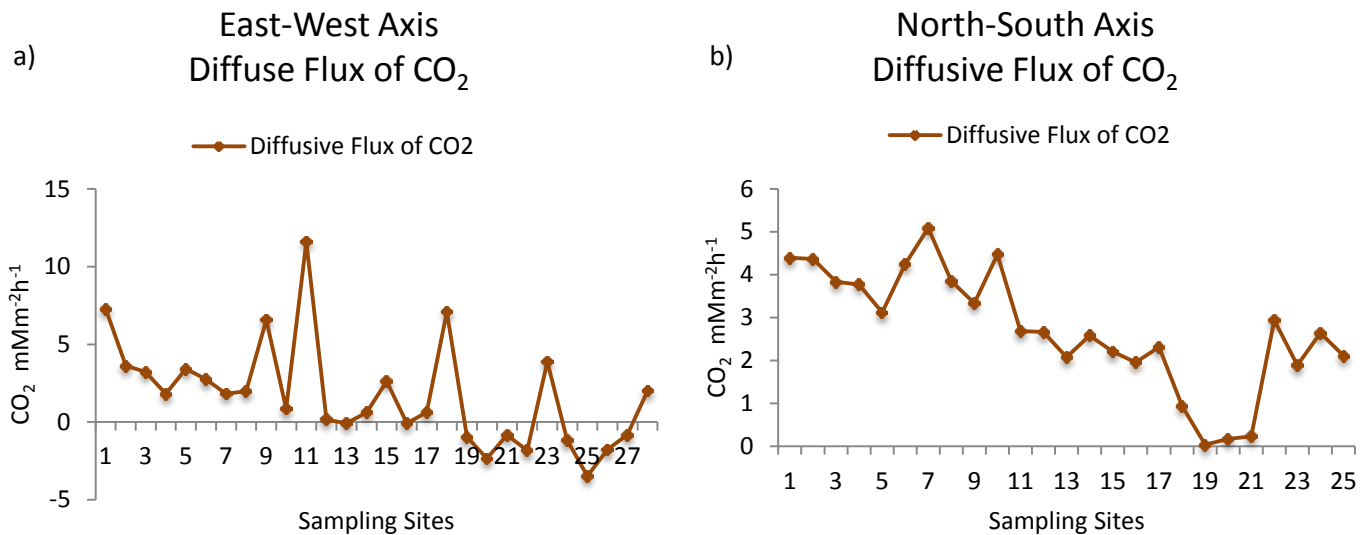


Figure 12. Carbon dioxide (CO<sub>2</sub>; mM.m<sup>-2</sup>.h<sup>-1</sup>) diffusive flux variations along the sampling sites of the East-West and North-South axes of the Paranaguá Estuarine Complex.

### 3.3. Estimate of carbon export to the coastal zone

The variability of the currents and current velocities for both the longitudinal (East-West Component) and transversal (North-South Component) component, as collected by the S4 Current Meter is shown in the figures 13 and 14, illustrating the pattern of the spring tidal currents in the northern and southern mouth of the system for the sampling period. The transport and circulation mechanisms inside the PEC are complex and controlled by wind forces, tides and freshwater discharge (UNCLES & STEPHENS, 1990).

The mean velocity of the ebb tide was 1.07m.s<sup>-1</sup> for the N-M of the PEC (Table 2), exporting a volume of water of 40,949.91m<sup>3</sup>.s<sup>-1</sup>, 269.66kg.s<sup>-1</sup> of Dissolved Organic Carbon and 182.45kg.s<sup>-1</sup> of Particulate Organic Carbon to the adjacent coastal zone. The flood tide, on the other hand, presented a mean velocity of 0.59m.s<sup>-1</sup>, importing 22,561.79m<sup>3</sup>.s<sup>-1</sup> of water, 133.78kg.s<sup>-1</sup> of DOC and 100.55kg.s<sup>-1</sup> of POC to the PEC. The resultant of these fluxes for the N-M is an exportation of 21.39kg of DOC and 8.30kg of POC per second.

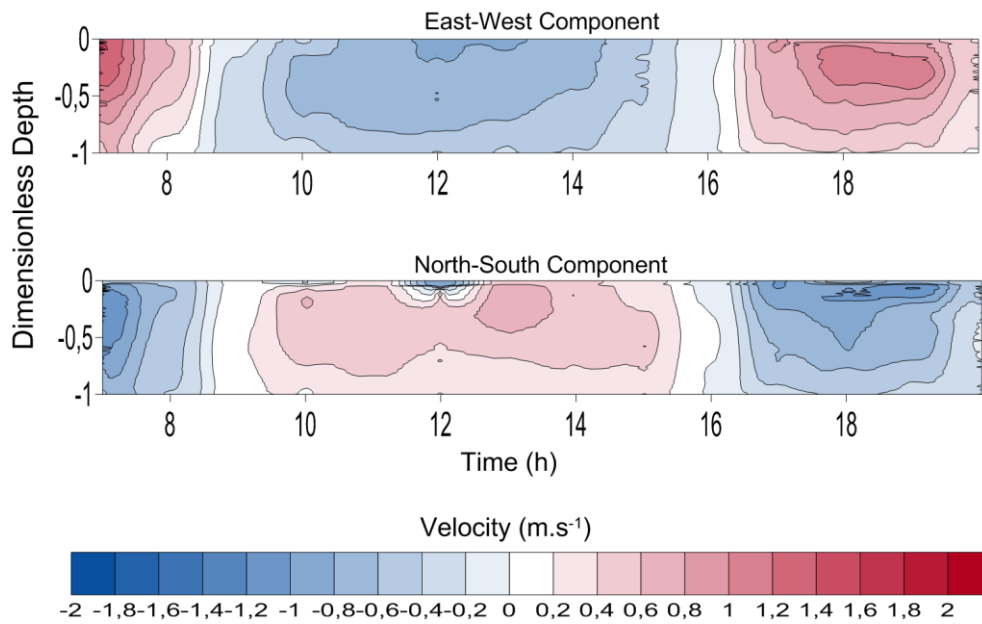


Figure 13. Velocity of the currents for the tidal cycle in the dimensionless depth at the Northern Mouth (figure 12a) - on 31/08/2012.

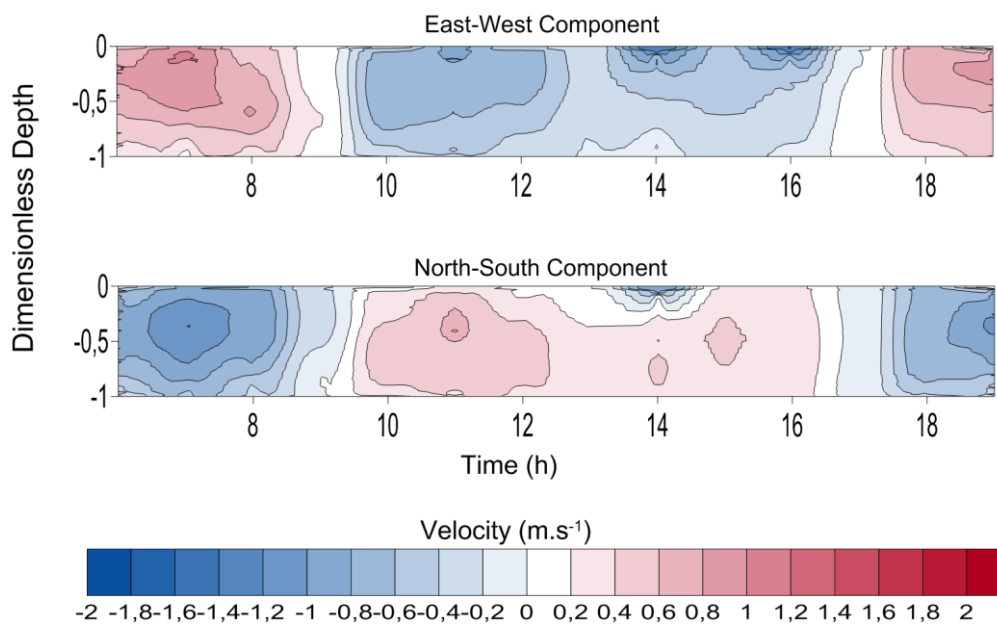


Figure 14. Velocity of the currents for the tidal cycle in the dimensionless depth at the Southern Mouth of the Paranaguá Estuarine Complex (figure 12b) - on 02/09/2012.

The S-M of the PEC presented for the ebb tide a mean velocity of  $0.77\text{m}\cdot\text{s}^{-1}$  (Table 2), exporting  $22,357.78\text{m}^3$  of water per second and showed a DOC and POC flux of  $81.55\text{kg}\cdot\text{s}^{-1}$  and  $170.07\text{kg}\cdot\text{s}^{-1}$ , respectively. The flood tide imported  $16,323.76\text{m}^3$  of water per second (mean velocity of  $0.56\text{m}\cdot\text{s}^{-1}$ ), giving the rise to a flux of  $72.81\text{kg}\cdot\text{s}^{-1}$  of DOC and  $96.73\text{kg}\cdot\text{s}^{-1}$  of POC to the PEC. For the S-M, the resultants showed that  $1.57\text{kg}\cdot\text{s}^{-1}$  of DOC were being imported from the adjacent ocean; and  $26.40\text{kg}\cdot\text{s}^{-1}$  of POC were being exported to the adjacent ocean. The present variation in OC transport along the tidal cycle can be due to the effect of tidal asymmetries, which are generated inside close systems as bays and estuaries, promoting residual current and tide-induced residual currents (MANTOVANELLI *et al.*, 2004)

The DOC exportation, during the sampling period for the PEC was higher than some riverine fluxes worldwide (Table 3). Moreover, our results are limited to a period of low precipitation rates (MARONE *et al.*, 1995). Rainy periods may change the observed behavior, since lower residence time of the water will increase the transportation rates of organic matter from the high to the lower sectors of the system and, therefore, the exportation to the adjacent coastal area.

Table 2. Mean values of Dissolved Organic Carbon (DOC), Particulate Organic Carbon (POC), water discharge, fluxes of DOC and POC during the ebb and flood tide for the two mouths of the Paranaguá Estuarine Complex – negative and positive values of fluxes represent fluxes towards the estuary and towards the adjacent ocean, respectively.

<b>Northern Mouth</b>	<i>DOC</i>	<i>POC</i>	<i>Water Discharge</i>	<i>Transportation of DOC</i>	<i>Transportation of POC</i>
	$\text{mg}\cdot\text{L}^{-1}$	$\text{mg}\cdot\text{L}^{-1}$	$\text{m}^3\cdot\text{s}^{-1}$	$\text{kg}\cdot\text{s}^{-1}$	$\text{kg}\cdot\text{s}^{-1}$
Ebb Tide	5.56	4.51	-40,949.91	-269.66	-182.45
Flood Tide	6.18	4.41	22,561.79	133.78	100.55

<b>Southern Mouth</b>	<i>DOC</i>	<i>POC</i>	<i>Water Discharge</i>	<i>Transportation of DOC</i>	<i>Transportation of POC</i>
	$\text{mg}\cdot\text{L}^{-1}$	$\text{mg}\cdot\text{L}^{-1}$	$\text{m}^3\cdot\text{s}^{-1}$	$\text{kg}\cdot\text{s}^{-1}$	$\text{kg}\cdot\text{s}^{-1}$
Ebb Tide	3.60	7.12	-22,357.78	-81.55	-170.07
Flood Tide	4.45	5.84	16,323.76	72.81	96.73

Table 3. Major worldwide riverine discharges ( $\text{m}^3 \cdot \text{s}^{-1}$ ), Dissolved and Particulate Organic fluxes ( $\text{kg} \cdot \text{s}^{-1}$ ) and global representativity of organic carbon input into the oceans.

Rivers	Riverine Discharge	DOC Flux	DOC Global Representativity	POC Flux	POC Global Representativity
	$\text{m}^3 \cdot \text{s}^{-1}$	$\text{kg} \cdot \text{s}^{-1}$	%	$\text{kg} \cdot \text{s}^{-1}$	%
<b>South America</b>					
Amazonas	183 283	605.66	7.64	412,23	7.39
Orinoco	34 881	142.69	1.8	63,42	1.14
Paraná	14 904	187.09	2.36	41,22	0.74
Uruguai	4 598	15.85	0.2	3,17	0.06
<u>Northern Mouth (PEC)</u>	<u>1 865</u>	<u>21.39</u>	<u>0.27</u>	<u>8.30</u>	<u>0.15</u>
<u>Southern Mouth (PEC)</u>	<u>1 529</u>	<u>-1.57</u>	<u>0</u>	<u>26.40</u>	<u>0.47</u>
<b>PEC</b>	<b>3394</b>	<b>19.82</b>	<b>0.25</b>	<b>34.70</b>	<b>0.62</b>
<b>North America</b>					
Mississippi	13 001	110.98	1.40	25,37	0.46
Columbia	5 771	12.68	0.16	7,93	0.14
St. Lawrence	13 096	49.15	0.62	9,83	0.18
Mackenzie	7 896	41.22	0.52	57,08	1.02
Yukon	6 659	28.54	0.36	9,51	0.17
Other US rivers - W coast	1 046	3.81	0.05	0,63	0.01
Other US rivers - E coast + Gulf of Mexico	5 676	16.17	0.20	47,56	0.85
<b>Africa</b>					
Zaire	41 223	321.85	4.06	25,37	1.59
Niger	4 820	16.81	0.21	7,93	0.38
Nile	1 205	6.02	0.08	9,83	0.22
Orange	349	0.95	0.01	57,08	0.01
Senegal	317	nd	nd	0,48	0.01
<b>Asia</b>					
Ob	13 730	62.79	0.79	38,05	0.68
Yenisei	17 599	95.13	1.20	53,91	0.97
Lena	16 013	114.16	1.44	57,08	1.02
Yellow	1 084	2.41	0.03	142,69	2.56
Yang Tse	29 332	57.08	0.72	158,55	2.84
Pearl	7 040	34.88	0.44	nd	nd
Ganges + Brahmaputra	30 790	114.16	1.44	1014,71	18.18
Indus	7 547	23.78	0.30	nd	Nd
<b>Europe</b>					
Danube	6 279	18.71	0.24	11,29	0.20
Po	1 471	3.81	0.05	4,44	0.08

Rhone	1 899	5.71	0.07	2,85	0.05
Loire	856	3.49	0.04	1,27	0.04
Garonne	679	2.38	0.03	1,11	0.02
Rhino	2201	nd	nd	11,73	0.21
<b><i>Measured*</i></b> <b><i>Rivers</i></b>	478 786	2117.77	26.96	2332.90	42.42
<b><i>Global</i></b> <b><i>Estimation</i></b>	1 119 356	7927.45	100	5580.92	100

\*Modified from Cauwet (2002). \*Measured rivers in which the exportations were calculated.

#### 4. CONCLUSION

The results presented in this work showed that for both axes (East-West and North-South), there was a pattern in terms of variation of CO<sub>2</sub> and O<sub>2</sub> saturation along the salinity gradient of the PEC; negative correlation between CO<sub>2</sub> and salinity contrasting with positive correlation between DO and salinity. The POC, DOC concentrations and light absorbance are highly variable, and together with the non-conservative behavior of the alkalinity, indicates several sources of organic matter to the system. Although, tests with Total Organic Carbon indicate that the same amount of organic carbon is available for the two axes, but in different phases for each axis – East-West Axis had 52% as POC while the North-South axis had 60% as DOC. The PCA analysis demonstrated an influence of the humic substances on the saturation of oxygen through its control on the availability of light for primary producers.

During the sampling period, the Paranaguá Estuarine Complex presented a heterotrophic metabolism, exporting CO<sub>2</sub> at the air-sea interface, in rates higher than several worldwide estuaries, along the East-West and North-South axes and the Northern and Southern Mouths. Contrasting with the two mouths of the PEC that presented autotrophic metabolism, importing CO<sub>2</sub> from the atmosphere. This difference might be due to the presence of mangrove systems, which exports high amounts of organic matter to the inner section of the PEC and the higher influence of marine water in the outer section of the PEC.

The exportations of DOC calculated herein for the two mouths of the PEC were higher than several major rivers around the world, indicating underestimation of the range in which carbon fluxes and organic carbon balances in the coastal zones. And based on the estimates of global carbon fluxes, the present work exhibits the importance of considering “local scales” system, as the PEC system in the global carbon balances.

## 5. REFERENCES

- ALVAREZ-SALGADO, X. A.; MILLER, A. E. J. 1998. Dissolved organic carbon in a large macrotidal estuary (the Humber, UK): Behaviour during estuarine mixing. *Mar. Pollut. Bull.*, 37: 216-224.
- AMON, R. M. W. & R. BENNER. 1994. Rapid cycling of high-molecular-weight dissolved organic matter in the ocean. *Nature*, 369: 549-552.
- ANGULO, R. J. 1992b. Geologia da planície costeira do Estado do Paraná. *Unpublished PhD thesis*. Instituto de Geociências de São Paulo. USP. 332 pg.
- ASMALA, E.; STEDMON, C. A.; THOMAS, D. N. 2012. Linking CDOM spectral absorption to dissolved organic carbon concentrations and loadings in boreal estuaries. *Estuarine, Coastal and Shelf Science*, 111: 107-117.
- BAUM, A.; T. RIXEN & J. SAMIAJI. 2007. Relevance of peat draining rivers in central Sumatra for the riverine input of dissolved organic carbon into the ocean. *Estuarine, Coastal and Shelf Science*, 73: 563-570.
- BENNER, R. & J. I. HEDGES. 1993. A test of the accuracy of fresh water DOC measurements by high-temperature catalytic oxidation and UV-promoted persulfate oxidation. *Marine Chemistry*, 41: 161-165.
- BENNER, R. & S. OPSAHL. 2001. Molecular indicator of the sources and transformations of dissolved organic matter in the Mississippi River plume. *Organic Geochemistry*, 32: 597-611.
- BIANCHI, T. S.; BAUER, J. E. 2011. Particulate Organic Carbon Cycling and Transformation. *In: Reference Module in Earth Systems and Environmental Sciences*, 5: 69-117.
- BLOUGH, N. V.; DEL VECCHIO, R. 2002. Chromophoric DOM in the Coastal Environment. In Hansell and Carlson (Eds). *Biogeochemistry of Marine Dissolved Organic Matter*. 509-546.
- BOEHM P. D. & J. G. QUINN. 1973. Solubilization of hydrocarbons by the dissolved organic matter in sea water. *Geochimica et Cosmochimica Acta*, 37: 2459-2477.
- BORGES, A. V.; ABRIL, G. 2012. Carbon Dioxide and Methane Dynamics in Estuary. *In: Treatise on Estuarine and Coastal Science*. Academic Press, 5: 119-161.
- BOWERS, D. G.; EVANS, D.; THOMAS, D. N.; ELLIS, K.; LE B. WILLIAMS, P. J. 2004. Interpreting the colour of an estuary. *Estuarine, Coastal and Shelf Science*, 59: 13-20.
- BOZEC, Y.; CARIOU, T.; MACÉ, E.; MORIN, P.; THUILLIER, D.; VERNET, M. 2012. Seasonal dynamics of air-sea CO<sub>2</sub> fluxes in the inner and outer Loire estuary (NW Europe). *Estuarine, Coastal and Shelf Science*, 100: 58-71.
- CARLSON, C. A. 2002. Production and Removal Processes. In Hansell and Carlson (Eds). *Biogeochemistry of Marine Dissolved Organic Matter*. 91-151.

- CARMOUZE, J-P. 1994. O Metabolismo dos Ecossistemas Aquáticos: Fundamentos teóricos, métodos de estudo e análises químicas. *FAPESP* 83-101.
- CAUWET, G.; GADEL, F.; DE SOUZA SIERRA, M. M.; DONARD, O.; EWALD, M. 1990. Contributions of the Rhone River to organic carbon inputs to the northwestern Mediterranean Sea. *Cont. Shelf Res.* 10: 1025-1037.
- CAUWET, G. 2002. DOM in the Coastal Zone. In: Hansell and Carlson (Eds). *Biogeochemistry of Marine Dissolved Organic Matter*. 579-609.
- CHEN, C. –T. A.; BORGES, A. V. 2009. Reconciling opposing views on carbon cycling in the coastal ocean: continental shelves as sinks and near-shore ecosystems as sources of atmospheric CO<sub>2</sub>. *Deep-Sea Res. II*, 56: 578–90.
- CHEN, C. –T. A.; HUANG, T. –H.; CHEN, Y. –C.; BAI, Y.; HE, X.; KANG, Y. 2013. Air-sea exchanges of CO<sub>2</sub> in the world's coastal seas. *Biogeosciences*, 10: 6509-6544.
- ELSE, B. G. T.; PAPAKYRIAKOU, T. N.; GRANSKOG, M. A.; YACKEL, J. J. 2008. Observations of sea surface fCO<sub>2</sub> distributions and estimated air-sea CO<sub>2</sub> fluxes in the Hudson Bay region (Canada) during the open water season. *Journal of Geophysical Research*, 113.
- FERRARI, G.M.; DOWELL, M.D.; GROSSI, S.; TARGA, C. 1996. The relationship between the optical properties of chromophoric dissolved organic matter and total concentration of dissolved organic carbon in the southern Baltic Sea region. *Marine Chemistry*, 55: 299–316.
- FERRARI, G.M.; DOWELL, M.D. 1998. CDOM absorption characteristic with relation to fluorescence and salinity in coastal areas of the Southern Baltic Sea. *Estuarine, Coastal and Shelf Science*, 47: 91–105.
- GRASSHOFF, K.; EHRHARDT, M.; KREMILING, K. (1983). *Methods of Seawater Analyses*, 2. ed., *Verlag Chemie*: Weinheim.
- GUO B.; J. SCHMITT, Z. CHEN, L. LIANG & J. F. MCCARTHY. 1994. Adsorption and desorption of natural organic matter on iron oxide: mechanisms and models. *Environmental Science and Technology*, 28: 38-46.
- HANSELL, D. A. & C. A. CARLSON. 1998b. Deep ocean gradients in dissolved organic carbon concentrations. *Nature*, 395: 263-266.
- HANSELL, D. A. & C. A. CARLSON. 2002. *Biogeochemistry of Marine Dissolved Organic Matter*. Ed. Elsevier *Science*: 774.
- HANSELLI, D. A.; D. KADKO & N. R. BATES. 2004. Degradation of terrigenous dissolved organic carbon in the Western Arctic Ocean. *Science*, 304: 858-861.
- HARVEY, G. R.; BORAN, D. A. 1985. Geochemistry of humic substances in seawater. In "Humic Substances in Soil, Sediment, and Water: Geochemistry, Isolation, and Characterization". Wiley-Interscience, New York.
- HEDGES, J. I. 1992. Global biogeochemical cycles: progress and problems. *Marine Chemistry*, 39: 67-93.
- HEDGES, J. I.; R. G. KEIL & R. BENNER. 1997. What happens to terrestrial organic matter in the ocean? *Organic Geochemistry*, 27: 195-212.
- HONG-GANG, NI.; FENG-HUI, LU.; XIAN-LIN, LUO.; HUI-YU, TIAN.; EDDY, Y.Z. 2008. Riverine inputs of total organic carbon and suspended particulate

- matter from the Pearl River Delta to the coastal ocean off South China. *Marine Pollution Bulletin*, 54: 1150-1157.
- HUNG, J.-J.; S.-M. WANG & Y.-L. CHEN. 2007. Biogeochemical controls on distributions and fluxes of dissolved and particulate organic carbon in the Northern South China Sea. *Deep-Sea Research II*, 54: 1486-1503.
- JEONG, S.; SATHASIVAN, A.; KASTL, G.; SHIM, W. G.; VIGNESWARAN, S. 2014. Experimental investigation and modeling of dissolved organic carbon removal by coagulation from seawater. *Chemosphere*, 95: 310-316.
- KALLE, K. 1938. Zum Problem des Meereswasserfarbe. *Ann. Hydrobiol. Mar. Mitt.*, 66: 1-13.
- KEMPE, S.; PETTINE, M.; CAUWET, G. 1991. Biogeochemistry of European rivers. In "Biogeochemistry of Major World Rivers". Wiley, Chichester: 168-211.
- KEIL, R. G.; MAYER, L. M.; QUAY, P. D.; RICHEY, J. E.; HEDGES, J. I. 1997. Loss of organic matter from riverine particles in deltas. *Geochim. Cosmochim. Acta* 61: 1507-1511.
- KHATIWALA, S.; TANHUA, T.; MIKALOFF FLETCHER, S.; GERBER, M.; DONEY, S. C.; GRAVEN, H. D.; GRUBER, N.; MCKINLEY, G. A.; MURATA, A.; RIOS, A. F.; SABINE, C. L. 2013. Global ocean storage of anthropogenic carbon. *Biogeosciences*, 10: 2169-2191.
- KIEBER R. J.; X. ZHOU & K. MOPPER. 1990. Formation of carbonyl compounds from UV-induced photodegradation of humic substances in natural waters: fate of riverine carbon in the sea. *Limnology and Oceanography*, 35: 1503-1515.
- KROM M. D. & E. R. SHOLKOVITZ. 1977. Nature and reactions of dissolved organic matter in the interstitial waters of marine sediments. *Geochimica et Cosmochimica Acta*, 41: 1565-1573.
- LAMOUR, M.R.; SOARES, C.R.; CARRILHO, J.C. 2004. Mapas de parâmetros texturais de sediment de fundo do Complexo Estuarino de Paranaguá – PR. *Boletim Paranaense de Geociências*, 55: 77-82.
- LEGENDRE, P.; LEGENDRE, L. 2012. Numerical Ecology Third Edition. Elsevier: 1006.
- LIBARDONI, B.G. 2012. Fluxos Fluviais de Carbono Orgânico Dissolvido para od Complexo Estuarino de Paranaguá, Paraná, Brasil. *Unpublished Bachelor Thesis*. Accessed on 14<sup>th</sup> January 2014, retrieved from: <http://dspace.c3sl.ufpr.br:8080/dspace/handle/1884/32378/browse?value=Libardoni%2C+Bruno+Guides&type=author>
- MANTOURA, R. F. C.; WOODWARD, E. M. S. 1983. Conservative behaviour of riverine dissolved organic carbon in the Severn estuary: Chemical and geochemical implications. *Geochim Cosmochim. Acta* 4, 1293-1309.
- MANTOVANELLI, A.; MARONE, E.; DA SILVA, E. T.; LAUTERT, L. F.; KLINGENFUSS, M.S.; PRATA JR., V. P.; NOERNBERG, M. A.; KNOPPERNS, B. A.; ANGULO, R. J. 2004. Combined tidal velocity and duration asymmetries as a determinant of water transport and residual flow in Paranaguá Bay estuary. *Estuarine, Coastal and Shelf Science*, 59: 523-537.
- MARONE, E.; M. R. GUIMARÃES, V. P. PRATA JR, M. S. KLINGENFUSS, R. CAMARGO, 1995. Caracterização física das condições oceanográficas,

- meteorológicas e costeiras das zonas estuarinas da Baía de Paranaguá, PR. VI Congresso Latinoamericano de Ciencias del Mar. Argentina.
- MARONE, E.; E. C. MACHADO, R. M. LOPES & E. T. SILVA. 2005. Land-Ocean fluxes in the Paranaguá Bay Estuarine System, Southern Brazil. *Brazilian Journal of Oceanography*, 53: 169-181.
- MARTINS, O.; PROBST, J. L. 1991. Biogeochemistry of major African Rivers: carbon and mineral transport. In "Biogeochemistry of Major World Rivers", Wiley, Chichester: 127-155.
- MEYERS-CHULTE, K. J. & J. I. HEDGES. 1986. Molecular evidence for a terrestrial component of organic matter dissolved in ocean water. *Nature*, 321: 61-63.
- MORA, A.; LARAQUE, A.; MOREIRA-TURCQ, P.; ALFONSO, J. A. 2014. Temporal variation and fluxes of dissolved and particulate organic carbon in the Apure, Caura, and Orinoco rivers, Venezuela. *Journal of South American Earth Sciences*, 54: 47-56.
- MOREIRA-TURCQ, P.; SEYLER, P.; GUYOT, J. L.; ETCHEBER, H. 2003. Exportation of organic carbon from the Amazon River and its main tributaries. *Hydrological Processes*, 17: 1329-1344.
- MUYLAERT, K.; DASSEVILLE, R.; DE BRABANDERE, L.; DEHAIRS, F.; VYVERMAN, W. 2005. Dissolved organic carbon in the freshwater tidal reaches of the Schelde estuary. *Estuarine, Coastal and Shelf Science*, 64: 591-600.
- NELSON, N. B.; SIEGEL, D. A.; 2002. Chromophoric DOM in the Open Ocea. In Hansell and Carlson (Eds). *Biogeochemistry of Marine Dissolved Organic Matter*. 547-578.
- NOERNBERG, M. A. 2001. Processos Morfodinâmicos no Complexo Estuarino de Paranaguá – Paraná – Brasil: um estudo a partir de dados in situ e Landsat – TM. *Unpublished Thesis*. PPGG, Universidade Federal do Paraná, Curitiba, 180.
- PAULA E. V. & C. CUNICO. 2007. O assoreamento das baías de Antonina e de Paranaguá e a gestão de suas bacias hidrográficas. In: *Dragagens Portuárias no Brasil. Antonina, Paraná*. 144-154.
- REGNIER, P.; FRIEDLINGSTEIN, P.; CIAIS, P.; MACKENZIE, F. T.; GRUBER, N.; JANSSENS, I. A.; LARUELLE, G. G.; LAUERWALD, R.; LUYSSAERT, S.; ANDERSSON, A. J.; ARNDT, S.; ARNOSTI, C.; BORGES, A. V.; DALE, A. W.; GALLEGOS-SALA, A.; GODDÉRIS, Y.; GOOSSENS, N.; HARTMANN, J.; HEINZE, C.; ILYINA, T.; JOOS, F.; LAROWE, D. E.; LEIFELD, J.; MEYSMAN, F. J. R.; MUNHOVEN, G.; RAYMOND, P. A.; SPAHNI, R.; SUNTHARALINGAM, P.; THULLNER, M. 2013. Anthropogenic perturbation of the carbon fluxes from land to ocean. *Nature geoscience*, 6: 597-607.
- RICHEY, J. E. 1991. The biogeochemistry of a major river system: the Amazon case study. In "Biogeochemistry of Major World Rivers", Wiley, Chichester: 57-74.
- ROCHA, J. C. & A. H. ROSA, 2003. In *Substâncias Húmicas Aquáticas: Interação com Espécies Metálicas*. 120p.

- SALIOT, A.; PARRISH, C. C.; SADOUNI, N. M.; BOULOUBASSI, I.; FILLAUX, J. I.; CAUWET, G. 2002. Transport and fate of Danube Delta terrestrial organic matter in the Northwest Black Sea mixing zone. *Marine Chemistry*, 79: 243–259.
- SEKI, O.; YOSHIKAWA, C.; NAKATSUKA, T.; KAWAMURA, K.; WAKATSUCHI, M. 2006. Fluxes, source and transport of organic matter in the western Sea of Okhotsk: stable carbon isotopic ratios of n-alkanes and total organic carbon. *Deep-Sea Research Part I: Oceanographic Research Papers*, 153: 253–270.
- SHARP, J. H.; PENNOCK, J. R.; CHURCH, T. M.; TRAMONTANO, J. M.; CIFUENTES, L. A. 1984. The estuarine interaction of nutrients, organics and metals: A case study in the Delaware Estuary. In: “*The Estuary as a Filter*”, V.S. Kennedy Ed. Academic Press, Orlando. 241-258.
- SPITZY, A. & V. ITTEKKOT. 1986. Gelbstoff: an uncharacterized fraction of dissolved organic carbon. In “The Influence of Yellow Substances on Remote Sensing of Seawater Constituents from Space”, Vol. 2, GKSS Geesthacht Research Center, Geesthacht, Germany, p. 31.
- STEDMON, C. A.; MARKAGER, S. S. 2003. Behaviour of optical properties of coloured dissolved organic matter under conservative mixing. *Estuarine, Coastal and Shelf Science*, 57: 973-979.
- TELANG, S. A.; POCKLINGTON, R.; NAIDU, A. S.; ROMANKEVITCH, E. A.; GITELSON, I. I.; GLADYSHEV, M. I. 1991. Carbon and minerals transport in major North American, Russian Arctic and Siberian Rivers: The St. Lawrence, the Mackenzie, the Yukon, the arctic Alaskan Rivers, the arctic basin rivers in the Soviet Union and the Yenisei. In “Biogeochemistry of Major World Rivers, SCOPE Report 42”, Wiley, Chichester: 75-104.
- THIMSEN C. A. & R. G. KEIL. 1998 Potential interactions between sedimentary dissolved organic matter and mineral surface. *Marine Chemistry*, 62: 65-76.
- VODACEK, A.; BLOUGH, N.V.; DEGRANDPRE, M.D.; PELTZER, E.T.; NELSON, R.K. 1997. Seasonal variation of CDOM and DOC in the Middle Atlantic Bight: terrestrial inputs and photooxidation. *Limnology and Oceanography* 42: 674–686.
- WANG, X.-C.; R. F. CHEN & G. B. GARDNER. 2004. Sources and transport of dissolved and particulate organic carbon in the Mississippi River estuary and adjacent coastal waters of the northern Gulf of Mexico. *Marine Chemistry*, 89: 241-256.
- WANG, Z. H. A.; CAI, W. J. 2004. Carbon dioxide degassing and inorganic carbon export from a marsh-dominated estuary (the Duplin River): a marsh CO<sub>2</sub> pump. *Limnology Oceanography*, 49: 341–54.
- WANNINKHOF, R.; PARK, G.-H.; TAKAHASHI, T.; SWEENEY, C.; FEELY, R.; NOJIRI, Y.; GRUBER, N.; DONEY, S. C.; MCKINGLEY, G. A.; LENTON, A.; LE QUÉREC, C.; HEINZE, C.; SCHWINGER, J.; GRAVEN, H.; KHATIWALA, S. 2013. Global ocean carbon uptake: magnitude, variability and trends. *Biogeosciences*, 10: 1983-2000.

- WHITEHOUSE, B. G.; R. W. MACDONALD, K. ISEKI, M. B. YUNKER & F. A. MCLAUGHLIN. 1989. Organic carbon and colloids in the Mackenzie River and Beaufort Sea. *Marine Chemistry*, 26: 371-378.
- WILLIAMS, P. M. & E. R. M. DRUFFEL. 1987. Radiocarbon in dissolved organic matter in the Central North Pacific Ocean. *Nature*, 330: 246-248.
- WOLLAST, R. 1993. Interactions of carbon and nitrogen cycles in the coastal zone. In: WOLLAST, R.; F. T. MACKENZIE & L. CHOU (Eds): Interactions of C, N, P and S Biogeochemical Cycles and Global Change. *Springer- Verlag Berlin Heidelberg*. NATO ASI Series I (4): 401-445.
- ZHAI, W.; DAI, M. 2009. On the seasonal variation of air-sea CO<sub>2</sub> fluxes in the outer Changjiang (Yangtze River) Estuary, East China Sea. *Marine Chemistry*, 117: 2-10.

## 6. APPENDIX

Location	Sample	Lat	Long	DTC	DOC	TC	TOC	PTC	POC	Abs_320	Abs_443	Temp °C	Salinity	pH	% DO	% CO2	Alc
Northern_Mouth	8	25°28'33,9''''	48°19'25,5''''	5,58	5,58	9,72	9,72	3,58	3,73	0,0623	0,0048	20	29	8	92,84	68,08	768,1
Northern_Mouth	9	25°28'33,9''''	48°19'25,5''''	6,51	6,51	10,48	10,48	4,9	4,9	0,0640	0,0054	20,5	29	8,02	102,63	44,89	546
Northern_Mouth	10	25°28'33,9''''	48°19'25,5''''	5,5	5,5	10,65	10,65	4,14	4,14	0,0575	0,0044	20,5	27	7,89	93,92	65,21	534
Northern_Mouth	11	25°28'33,9''''	48°19'25,5''''	5,28	5,28	9,77	9,77	4,27	4,27	0,0525	0,004	21	29	8,01	98,11	46,93	553,4
Northern_Mouth	12	25°28'33,9''''	48°19'25,5''''	5,72	5,72	10,78	10,78	5,5	5,5	0,0507	0,0038	21	25	7,98	94,26	63,84	627,5
Northern_Mouth	13	25°28'33,9''''	48°19'25,5''''	5,74	5,74	10,47	10,47	4,75	4,75	0,0483	0,0034	21	26	8,04	92,71	48,62	578,3
Northern_Mouth	14	25°28'33,9''''	48°19'25,5''''	6,72	6,72	12,33	12,33	6,59	6,59	0,0433	0,0033	21	30	8,04	96,53	46,26	602,8
Northern_Mouth	15	25°28'33,9''''	48°19'25,5''''	6,67	6,67	9,12	9,12	2,4	2,4	0,0391	0,0026	20,5	31	8,05	102,1	38,9	540,1
Northern_Mouth	16	25°28'33,9''''	48°19'25,5''''	7,29	7,29	8,87	8,87	2,2	2,2	0,0400	0,0023	20,5	30	8,07	95,49	39,06	558,5
Northern_Mouth	17	25°28'33,9''''	48°19'25,5''''	7,08	7,08	12,7	12,7	5,41	5,41	0,0442	0,0032	20,5	29	8,05	91,51	41,29	546
Northern_Mouth	18	25°28'33,9''''	48°19'25,5''''	7,12	7,12	10,57	10,57	3,49	3,49	0,0536	0,0038	20,5	29	8,05	95,2	40,3	534
Northern_Mouth	19	25°28'33,9''''	48°19'25,5''''	7,04	7,04	11,13	11,13	4,01	4,01	0,0522	0,0038	20	30	8,04	91,06	41,99	553,4
Northern_Mouth	20	25°28'33,9''''	48°19'25,5''''	10,15	9,99	13,48	13,48	6,44	6,44	0,0547	0,0039	20	30	8,05	98,24	38,57	525,3
North-South	1	25°15'48,2''''	48°20'09,8''''	8,09	8,09	15,26	15,26	5,11	5,27	0,0951	0,0046	19	20	7,44	71,35	303,8	708,1
North-South	2	25°15'55,1''''	48°19'58,7''''	19,37	19,37	13,05	13,05	4,96	4,96	0,0948	0,0049	19	20	7,44	74,71	302,6	705,3

North-South	3	25°16'15,7""	48°19'51,6""	8,04	8,04	21,41	21,41	2,04	2,04	0,0958	0,005	19	20	7,48	73,54	262,7	674,2
North-South	4	25°16'32,8" "	48°19'51,8""	7,11	7,11	15,61	15,61	7,57	7,57	0,0951	0,0049	19	20	7,47	72,37	263,6	660,6
North-South	5	25°17'04,5""	48°19'51,8""	6,02	6,02	12,55	12,55	5,44	5,44	0,0942	0,0048	19	20	7,5	72,02	226,5	610,7
North-South	6	25°17'49,4""	48°19'54,5""	7,49	7,49	15,21	15,21	9,19	9,19	0,0918	0,0054	19	21	7,52	74,87	262	753,5
North-South	7	25°18'19,4""	48°19'54,7""	8,22	8,22	16,87	16,87	9,38	9,38	0,0905	0,0045	19	20	7,57	76,92	276,4	878,3
North-South	8	25°18'47,5""	48°19'58,0""	9,24	9,24	13,47	13,47	5,25	5,25	0,0917	0,0054	19	20	7,59	78,67	227,6	760,6
North-South	9	25°19'12,3""	48°20'02,3""	10,22	10,22	15,53	15,53	6,29	6,29	0,0881	0,0044	19	21	7,63	80,66	199,2	748,4
North-South	10	25°19'39,8""	48°20'08,9""	14,62	14,62	17,42	17,42	7,2	7,2	0,0861	0,0043	19	21	7,67	78,8	221,4	914,4
North-South	11	25°19'52,6""	48°20'12,8""	6,51	6,51	16,82	16,82	2,2	2,2	0,0856	0,0044	19	23	7,67	78,05	170,5	734,7
North-South	12	25°20'10,6""	48°20'16,5""	6,65	6,65	15,15	15,15	8,64	8,64	0,0818	0,0039	19	23	7,72	80,43	162,3	790,3
North-South	13	25°20'32,4""	48°20'18,2""	11,28	11,28	12,73	12,73	6,08	6,08	0,0809	0,0035	19	24	7,74	82,05	145,6	760,9
North-South	14	25°20'55,3""	48°20'23,8""	12,76	12,76	16,5	16,5	5,22	5,22	0,0830	0,0031	19	24	7,72	81,48	159,4	791,6
North-South	15	25°21'25,9""	48°20'31,8""	5,44	5,44	18,31	18,31	5,55	5,55	0,0801	0,0027	19	25	7,74	87,05	147,6	786
North-South	16	25°22'07,4""	48°20'36,8""	8,08	8,08	12,33	12,33	6,89	6,89	0,0787	0,0024	19	24	7,77	84,76	140	788,3
North-South	17	25°22'53,5""	48°20'41,4""	6,22	6,22	16,5	16,5	8,42	8,42	0,0746	0,0021	19	25	7,82	86,04	141,4	917,6
North-South	18	25°23'32,6""	48°20'51,4""	6,18	6,18	13,86	13,86	7,64	7,64	0,0863	0,0049	19	27	7,84	87,39	115,5	823,8
North-South	19	25°24'29,1""	48°21'01,3""	12,57	12,57	13,12	13,12	6,94	6,94	0,0721	0,0017	19	29	7,88	75,98	100,5	827,5

South																		
North-South	20	25°25'24,7'''''	48°21'03,3'''''	9,56	9,56	16,89	16,89	4,32	4,32	0,0746	0,0015	19	27	7,88	83,42	102,5	843,6	
North-South	21	25°26'10,3'''''	48°20'58,1'''''	5,49	5,49	12,17	12,17	2,61	2,61	0,0710	0,001	18,5	28	7,9	85,99	103,2	878,3	
North-South	22	25°26'55,5'''''	48°20'46,3'''''	4,16	4,16	9,88	9,88	4,39	4,39	0,0669	0,0004	18,5	29	7,68	86,58	167,8	833,6	
North-South	23	25°27'27,5'''''	48°20'24,1'''''	10,77	10,77	8,3	8,3	4,14	4,14	0,0649	0,0004	18,5	30	7,78	88,73	133,9	871,4	
North-South	24	25°27'46,5'''''	48°20'09,8'''''	5,96	5,96	15,68	15,68	4,91	4,91	0,0739	0,0016	18	29	7,73	83,39	153	880,9	
North-South	25	25°28'12,9'''''	48°19'44,1'''''	4,8	4,8	9,05	9,05	3,09	3,09	0,0612	-0,0011	18	29	7,77	86,37	139,2	869,9	
Southern_Mouth	7	20°32,7'75,9'''''	48°21,9'69'''''	3,09	2,94	7,13	7,13	2,33	2,33	0,0317	0,0023	20	32	8,19	96,79	26,98	574,2	
Southern_Mouth	8	20°32,7'75,9'''''	48°21,9'69'''''	3,5	3,32	8,98	8,98	5,56	5,75	0,0480	0,0044	20,5	32	8,21	95,2	24,74	560,6	
Southern_Mouth	9	20°32,7'75,9'''''	48°21,9'69'''''	3,57	3,42	9,17	9,17	6,08	6,23	0,0493	0,0042	21	28	8,23	96,37	30,4	646	
Southern_Mouth	10	20°32,7'75,9'''''	48°21,9'69'''''	6,99	6,24	10,09	10,09	6,59	6,77	0,0481	0,0042	22	25	8,25	96,41	27,73	551,6	
Southern_Mouth	11	20°32,7'75,9'''''	48°21,9'69'''''	3,54	3,33	8,16	8,16	4,59	4,74	0,0413	0,0029	21	26	8,29	94,39	29,25	698,2	
Southern_Mouth	12	20°32,7'75,9'''''	48°21,9'69'''''	4,78	4,78	13,02	13,02	6,03	6,78	0,0365	0,0023	21	28	8,31	96,5	21,42	586	
Southern_Mouth	13	20°32,7'75,9'''''	48°21,9'69'''''	3,49	3,49	11,62	11,62	8,08	8,29	0,0313	0,0018	21	29	8,34	96,84	18,97	586,1	
Southern_Mouth	14	20°32,7'75,9'''''	48°21,9'69'''''	9,17	4,64	8,39	8,39	3,61	3,61	0,0315	0,0017	20,5	30	8,35	99,43	18,03	591,2	
Southern_Mouth	15	20°32,7'75,9'''''	48°21,9'69'''''	4,94	4,59	9,27	9,27	5,78	5,78	0,0277	0,0009	20,5	31	8,37	99,51	16,08	580,9	
Southern_Mouth	16	20°32,7'75,9'''''	48°21,9'69'''''	4,1	4,1	13,15	13,15	3,98	8,51	0,0308	0,0018	20,5	31	7,9	99,37	61,57	563,2	

Southern_Mouth	17	20°32,7'75,9""	48°21,9'69""	3,41	3,41	8,25	8,25	3,31	3,66	0,0238	0,0001	20,1	33	7,92	101,02	56,24	568,1
Southern_Mouth	18	20°32,7'75,9""	48°21,9'69""	3,5	3,5	8,37	8,37	4,27	4,27	0,0260	0,0009	20,1	31	7,86	99,05	66,15	546
Southern_Mouth	19	20°32,7'75,9""	48°21,9'69""	5	5	8,89	8,89	5,48	5,48	0,0332	0,002	20,1	31	7,84	98,9	72,11	563,4
East-West	1	25°24'04,6""	48°43'49,8""	11,87	11,87	15,79	15,79	12,29	12,29	0,1193	0,0167	17	15	7,49	76,54	420,8	1025
East-West	2	25°24'28,3""	48°42'54,2""	3,94	3,94	12,23	12,23	7,23	7,23	0,1155	0,0131	17	18	7,55	79,45	232,7	695,1
East-West	3	25°26'06,3""	48°42'06,6""	3,88	3,88	20,48	20,48	8,61	8,61	0,1049	0,0078	17	18	7,62	78,76	200,8	709,8
East-West	4	25°26'48,4""	48°41'01,5""	6,44	6,44	9,45	9,45	5,51	5,51	0,1008	0,0076	17	23	7,75	84,82	138,6	742,3
East-West	5	25°27'33,1" "	48°40'08,8""	4,24	4,24	12,92	12,92	9,04	9,04	0,0992	0,0073	17	24	7,74	78,96	173,4	919,8
East-West	6	25°28'15,2" "	48°39'16,7""	3,84	3,84	14,73	14,73	8,29	8,29	0,0988	0,0087	17	25	7,8	83,53	150,5	945,1
East-West	7	25°28'36,6""	48°38'43,2""	6,88	6,88	12,71	12,71	8,47	8,47	0,0953	0,0076	17	25	7,8	89,42	133,4	840,3
East-West	8	25°28'43,3""	48°38'15,6""	4,55	4,55	12,1	12,1	8,26	8,26	0,0964	0,0082	17	25	7,85	86,46	132,3	942,3
East-West	9	25°29'02,7""	48°37'19,6""	5,75	5,75	14,69	14,69	7,81	7,81	0,0935	0,0044	17	25	7,82	87,31	215,1	1410
East-West	10	25°29'13,5""	48°36'46,1""	5,72	5,72	12,23	12,23	7,68	7,68	0,0891	0,0038	17	25	7,88	86,03	113,1	871,4
East-West	11	25°29'23,8""	48°35'58,9""	5,16	5,16	10,94	10,94	5,19	5,19	0,0889	0,0042	17	26	7,37	86	656,6	1467
East-West	12	25°29'27,5""	48°34'57,2""	13,08	13,08	13,08	13,08	7,36	7,36	0,0859	0,0037	17	26	7,91	85,81	102,1	867,5
East-West	13	25°29'30,6""	48°34'09,4""	4,04	4,04	13,5	13,5	8,34	8,34	0,0868	0,0042	17	27	7,91	84,67	99,01	858,6
East-West	14	25°29'36,1" "	48°32'51,6""	4,63	4,63	17,58	17,58	4,5	4,5	0,0857	0,0044	17	27	7,87	87,17	109,2	854,3
East-West	15	25°29'38,5""	48°32'08,3""	5,36	5,36	8,46	8,46	4,42	4,42	0,0839	0,0037	17	28	7,84	86,53	141,5	1040
East-West	16	25°29'42,3""	48°30'53,0""	4,71	4,71	7,77	7,77	3,14	3,14	0,0967	0,0059	17	29	7,9	84,12	99,08	871,4
East-West	17	25°29'43,3""	48°30'03,6""	3,96	3,96	12,43	12,43	7,07	7,07	0,0958	0,0056	17	29	7,87	79,01	109,2	888
East-West	18	25°29'41,9""	48°29'20,4""	5,49	5,31	10,65	10,65	5,94	5,94	0,0912	0,0048	17	29	7,92	84,28	191,6	1742
East-West	19	25°29'45,7" "	48°28'26,8""	6,97	6,97	10,76	10,76	6,8	6,8	0,0902	0,0046	17	29	7,97	86,33	89,05	938
East-West	20	25°29'50,4""	48°27'36,8""	10,07	10,07	12,1	12,1	6,61	6,79	0,0754	0,0027	17	29	8	85,86	75	858,6
East-West	21	25°29'57,5""	48°26'22,6""	10,41	10,41	9,8	9,8	2,83	2,83	0,0725	0,0033	17	30	7,94	87,75	89,92	895,1
East-West	22	25°30'03,7""	48°25'45,8""	5,32	5,15	16,95	16,95	6,88	6,88	0,0728	0,0024	17	30	7,99	87,4	80,55	914,4
East-West	23	25°30'12,2""	48°25'07,3""	5,83	5,83	15,5	15,5	5,09	5,09	0,0719	0,0046	17	30	8,02	91,99	138,7	1671
East-West	24	25°30'36,4""	48°24'15,1""	13,56	13,56	14,11	14,11	8,79	8,96	0,0677	0,004	17	30	8,03	91,85	88,6	1110

East-West	25	25°31'22,0""	48°23'05,4""	7,02	7,02	12,25	12,25	6,42	6,42	0,0560	0,0009	17	30	8,05	88,74	67,91	906
East-West	26	25°32'13,8""	48°22'17,4""	10,27	10,27	23,33	23,33	9,77	9,77	0,0519	0,00005	17	30	8,05	89,98	83,66	1106
East-West	27	25°32'57,5""	48°21'46,0""	4,12	4,12	12,25	12,25	5,23	5,23	0,0551	0,0011	17	30	8,03	85,04	92	1151
East-West	28	25°33'40,1""	48°21'09,2""	7,65	7,65	19,34	19,34	9,07	9,07	0,0507	-0,0001	17	30	7,88	91,91	128	1083